2

2. REPORT DATE	3. REPORT TYPE AND DATES COVERED
27 Feb 92	Final Report 1 Apr 88 to 31 Aug 91

4. TITLE AND SUBTITLE

Processing and Properties of Chemically Derived Calcium Silicate Cements

5. FUNDING NUMBERS

2306/A2 61102F

6. AUTHOR(S)

B. E. Scheetz, J. J. Mecholsky, and J. H. Adair

7. PERFORMING ORGANIZATION NAME(S) AND ADDRESS(ES)

Pennsylvania State University
248 Calder Way - Suite 300
University Park, PA 16802

8. PERFORMING ORGANIZATION REPORT NUMBER

AFOSR-TR- 92 0223

9. SPONSORING MONITORING AGENCY NAME(S) AND ADDRESS(ES)

AFOSR/NE
Building 410, Bolling AFB DC
20332-6448

10. SPONSORING MONITORING AGENCY REPORT NUMBER

AFOSR-88-0184

11. SUPPLEMENTARY NOTES

12a. DISTRIBUTION AVAILABILITY STATEMENT

APPROVED FOR PUBLIC RELEASE; DISTRIBUTION IS UNLIMITED.

12b. DISTRIBUTION CODE

13. ABSTRACT (Maximum 200 words)

chemical engineering approach has been employed to promote elimination of large-size flaws and improve strength. A general philosphy in the program was to prepare advanced cements designated as chemically bonded ceramics and use fracture mechanics and fractography to determine the size and origin of the critical flaw. Critical flaws of a certain type were eliminated in subsequent materials by alteration in some stage of the processing scheme. One of the most important goals of the current program was to analyze the effectiveness of indentation techniques for evaluating the mechanical properties of cementitious materials. The indentation-strength technique was found applicable to MDF cements for measuring fracture toughness. The indentation-strength technique and fracture surface analysis were found applicable to MDF cements for measuring fracture toughness. By using both optical and electron microscopes, fractography becomes a powerful tool to estimate the toughness. Therefore we suggest the small crack techniques are applicable for the measurement of crack growth resistance in cementitious materials as long as the crack size is larger than a characteristic dimension of the microstructure.

14. SUBJECT TERMS

15. NUMBER OF PAGES

89

16. PRICE CODE

17. SECURITY CLASSIFICATION OF REPORT	18. SECURITY CLASSIFICATION OF THIS PAGE	19. SECURITY CLASSIFICATION OF ABSTRACT	20. LIMITATION OF ABSTRACT
UNCLASSIFIED	UNCLASSIFIED	UNCLASSIFIED	

DISCLAIMER NOTICE

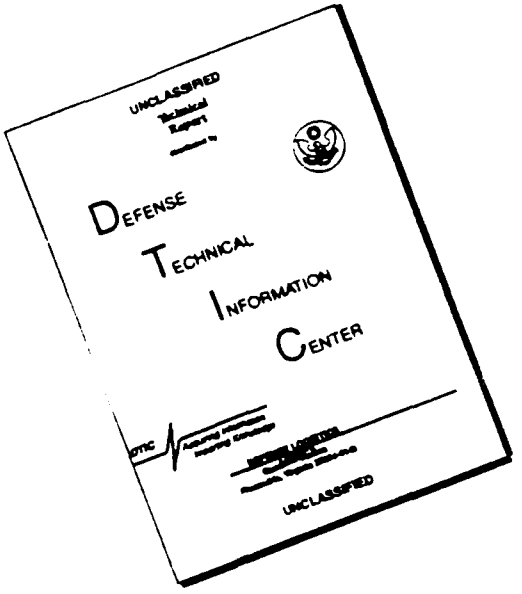

THIS DOCUMENT IS BEST QUALITY AVAILABLE. THE COPY FURNISHED TO DTIC CONTAINED A SIGNIFICANT NUMBER OF PAGES WHICH DO NOT REPRODUCE LEGIBLY.

4

PROCESSING AND PROPERTIES OF CHEMICALLY DERIVED CALCIUM SILICATE CEMENTS

Final Report for the Period

April 1, 1989 through August 31, 1991

Air Force Grant No. AFOSR-88-0184

Prepared for

AIR FORCE OFFICE OF SCIENTIFIC RESEARCH
ELECTRONIC AND MATERIAL SCIENCES DIRECTORATE

Principal Investigators:

B.E. Scheetz

The Pennsylvania State University

J.J. Mecholsky
J.H. Adair

University of Florida

February 20, 1992

TABLE OF CONTENTS

SUMMARY OF RESULTS

INTRODUCTION

Calcium silicate cements are the basis for the most widely used material in the world with ordinary Portland cement OPC) the structural material of choice for buildings, highways, bridges, and most of the other large structures in our everyday surroundings. OPC is usually mixed with enough water to be flowable such that near net shaping via casting is possible. A typical water to cement mass ratio (w/c) is 0.4. However, this level of water necessary to produce a castable cement paste is much greater than that required merely for the hydration of the cement precursor and residual water remains in the microstructure compromising mechanical properties. It has been shown that cements with greater strengths can be achieved by reducing the amount of water below a w/c of about 0.2 but these cements are often not flowable enough to be cast and must be formed via shear intensive operations such as extrusion or uniaxial pressing which limits the shapes that can be formed. Therefore, the long term objective of our work is to produce high strength calcium silicate cements without compromising the ability to use near net shape forming techniques.

The maximum compressive and flexural strengths for cement paste have been produced by Roy and Gouda (1975) at the Materials Research Laboratory at Penn State and Kendall et. al (1983-88) of the Imperial Chemical Company, respectively. Successive processing iterations have led to compressive strengths as high as 655 MPa (Roy and Gouda) and flexural strengths up to 250 MPa (Kendall et. al). The key to the development of high strength cements has been the elimination of microstructural flaws through increasingly more rigorous and carefully controlled processing iterations to reduce the size of critical flaws. Processing iterations have increased strength primarily by eliminating residual porosity. The work by Roy and Gouda (1975) underscored the effect that elimination of large crack-like flaws can have on improving strength and set the stage for the later studies by researchers at the Imperial Chemical Company (Birchall and coworkers including Kendall) to produce significant advances in flexural strength.

In the present study, a chemical engineering approach has been employed to promote elimination of large size flaws and improve strength. A general philosphy in the program was to prepare advanced cements designated as chemically bonded ceramics and use fracture mechanics and fractography to determine the size and origin of the critical flaw. Critical flaws of a certain type were eliminated in subsequent materials by alteration in some stage of the processing scheme.

The processing iterations with improvements in flexural strengths and fracture toughness for samples produced on this program are shown in Figure 1. Chou and Mecholsky (1990) have established that a fracture toughness test and flexural strength determination that also provides

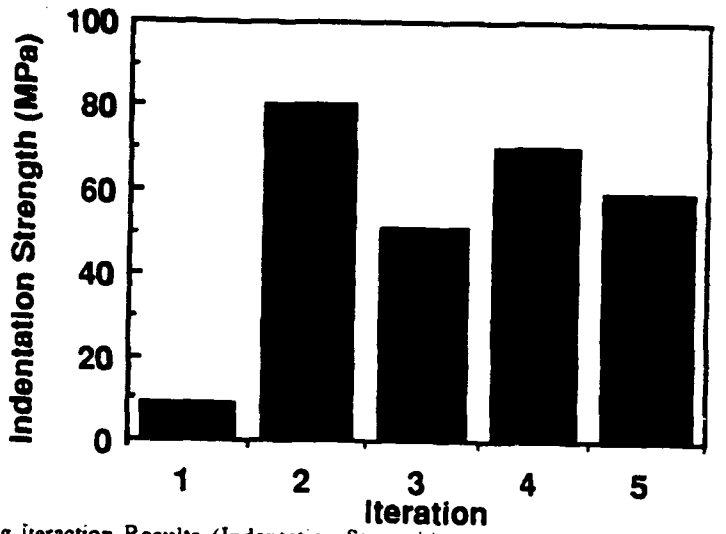

Processing Iteraction Results (Indentation Strength)
1. Conventional Cement
2. MDF OPC-Aloxide Derived Calcium Silicate
3. Gel-cast OPC - Hand Mixed
4. Gel-cast OPC - Shear Mixed
5. Gel-cast - Dehydrated Hydrothermally Derived Tobermorite

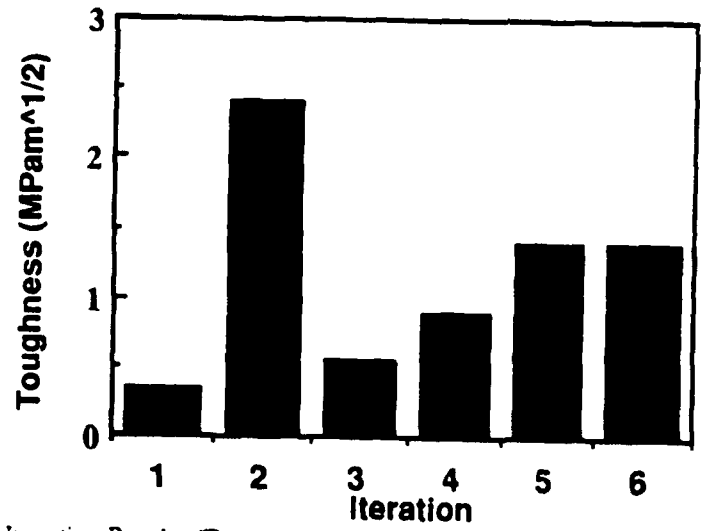

Processing Iteraction Results (Toughness)
1. Conventional Cement
2. MDF OPC-Aloxide Derived Calcium Silicate
3. MDF Cured Without Water
4. MDF Cured in Water
5. Gel-cast OPC Cured in Water
6. Gel-cast - Dehydrated Hydrothermally Derived Tobermorite

Figure 1. Processing Iterations Performed to Date with Flexural Strength and Toughness Achieved for each Iteration.

the critical flaw size, originally developed for advanced ceramics, can also be used for the chemically bonded materials in this program (see Appendices I and II). It can be seen that flexural strength has been improved from less than 10 MPa to about 80 MPa for the highest strength material. Likewise, fracture toughness has been improved from 0.3 $MPa \cdot m^{1/2}$ up to almost 2.5 $MPa \cdot m^{1/2}$ for the second iteration. The maximum fracture toughness achieved without the addition of a dispersed phase was 1.5 $MPa \cdot m^{1/2}$. Thus, dramatic mechanical property improvement has been achieved using the iterative approach.

The processing innovations that we are using on the program include advanced synthesis techniques for the CBC precursor powders, incorporation of surface chemical principles to enhance forming and chemical bonding of the materials, advanced forming techniques to both refine microstructure and produce unique shapes (e.g., substrates, guides, etc.), and the use of rigorous fracture mechanics analyses and fractography to analyze critical flaws and microstructures. Of these three areas of innovation, we believe that the results on the advanced synthesis, the surface chemistry, and the fractography will have the greatest impact on the general enhancement of CBC strength. However, the advanced forming techniques also will have a major role to play in ensuring that high strengths are achieved while still ensuring formability.

The progress on each of these research areas is presented. First, the evaluation of mechanical property determinations based on indentation techniques for cementitious materials is reviewed followed by the processing property iterations tested during the current reporting period. Some conclusions may be drawn that indicate the directions for current and future studies.

MECHANICAL PROPERTY AND CRITICAL FLAW DETERMINATIONS ON CBC MATERIALS

One of the most important goals of the current program was to analyze the effectiveness of indentation techniques for evaluating the mechanical properties of cementitious materials. Indentation techniques were combined with fracture surface analysis techniques, i.e., identifying the critical crack size and calculating the fracture toughness, in order to obtain comparative values with small crack techniques (see also Appendices I and II). The emphasis on small crack techniques is important because failure of reasonably good macro-defect-free (MDF) cements will have cracks smaller than 200 μm and of approximately the same shape as indentation-induced cracks.

The indentation-strength technique was found applicable to MDF cements for measuring fracture toughness[1]. A strength-indent load graph is shown in Figure 2. This graph demonstrates that the indentation theory developed for glass and polycrystalline ceramics is consistent with the data for MDF cements. This was the first time that the strength-indentation technique has been applied to cements. However, attempts have been made to apply crack-indentation techniques to

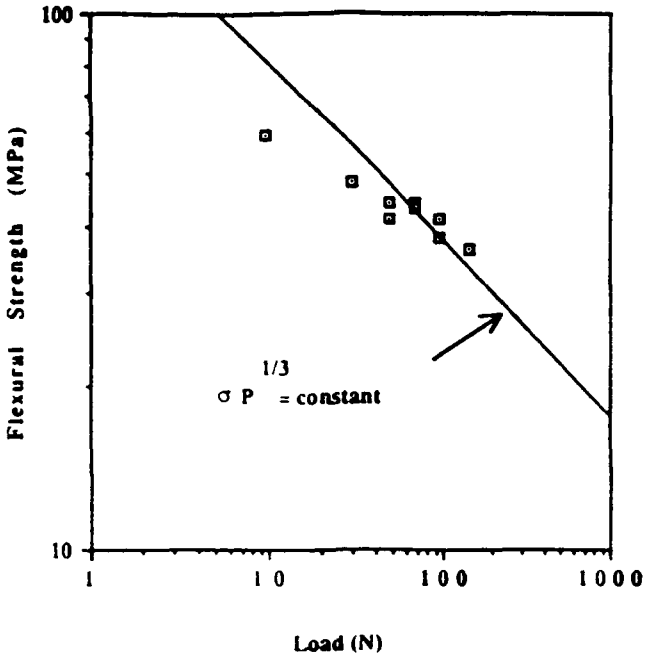

Figure 2. Flexural strength versus indent load is consistent with a -1/3 slope at high indent loads.

cement pastes with limited success[2]. The previous work[2] gained qualitative insight into fracture mechanisms, but did not attempt quantitative determination of the fracture toughness from the indentation impressions. By using both optical and electron microscopes, fractography becomes a powerful tool for estimating the toughness. The two techniques give comparable values (Table 1). We suggest that small crack techniques are applicable for the measurement of crack growth resistance in cementitious materials as long as the crack size is larger than a characteristic dimension of the microstructure (e.g., larger than an equivalent "grain size"). R-curve (crack growth resistance dependence on crack size) behavior was observed and the (apparent) toughness was about 1.25 $MPam^{1/2}$. Microcracking is suggested as a possible toughening mechanism for this MDF cement which was fabricated from OPC, 14 parts of deionized water and 3 parts polymer (polyacrylamide). Current processing techniques limit the study of the fracture process and toughening mechanisms.

Table 1. Test data for MDF cement.

#	Load (Kg)	$K_c(1)$ (MPa $m^{1/2}$)	$K_c(2)$ (MPa $m^{1/2}$)	c (μm)	σ (MPa)
1	1	1.00	1.08	119	59
2	3	1.14	1.12	200	48
3	3	0.95	---	---	38
4	5	1.13	1.18	305	41
5	5	1.20	1.11	234	44
6	7	1.24	1.04	237	41
7	7	1.28	1.29	329	43
8	10	1.35	1.25	341	41
9	10	1.28	1.36	497	38
10	15	1.35	1.32	498	36

--- = Flaw was not identified, c = Flaw Size, σ = Flexure Strength.

$K_c(1)$ is calculated using the indentation-strength technique.

$K_c(2)$ is calculated using fracture surface analysis.

Flaw size $c = (ab)^{1/2}$, where a is the depth of the semi-elliptical flaw and 2b is the width of the flaw on the surface.

PARTICLE SYNTHESIS AND CHARACTERIZATION

A major objective in the research was to chemically synthesize a fine particle calcium silicate which could be dehydrated and rehydrated to be used to produce a cement product with high bend strength. The particle size for OPC ranges from submicron to ~100μm and fracture analyses by Kendall et al. indicate that large, unhydrated grains are at least one source of critical flaws in these materials. Chemically derived calcium silicate was synthesized using both metal organic decomposition (MOD) and hydrothermal methods. The chemically derived, fine particles were then used to produce cements by extrusion and pressing. The basic procedure used to prepare caclium silicate powders by MOD is summarized in Appendix III and details are provided in the thesis whose abstract is Appendix IV.

An initial problem with the MOD method was low yield (3g/week). However, even after yields had been improved, the dried, MOD powder had a very large surface area (>100 m^2/g) and also a rather large mean particle size (5 μm) indicating the presence of agglomerates. Hard agglomerates in the MOD synthesized powder were confirmed in SEM photomicrographs. In an attempt to eliminate the agglomerates, the powder was milled. However, the powder reacted with the toluene used in milling and the mean particle size actually increased (9 μm). Furthermore, MOD powders could not be produced in an agglomerate-free state even with dispersant incorporated in the synthesis chamber.

The second powder preparation method evaluated was hydrothermal synthesis. This method was used in order to produce a well-crystallized, calcium silicate hydrate powders. After the method was fully developed, the dried powders had a specific surface areas from 20 to 50 m^2/g and consisted of either platelets (tobermorite, $5CaO{\cdot}6SiO_2{\cdot}5H_2O$) or acicular particles (xonotlite, $6CaO{\cdot}6SiO_2{\cdot}2H_2O$). Surface areas were not as large as those for the powders prepared by MOD, but it was determined by SEM that the particles were not agglomerated. Therefore, the hydrothermally synthesized tobermorite and xonotlite in both the dehydrated and as-synthesized state was used in subsequent processing iterations.

The hydrothermally derived tobermorite and xonotlite consisted of well-crystallized particles with predominantly a platy habit in the former and acicular habit in the latter materials. Each of these particles were characterized with respect to their likely crystallographic habit (Appendix V).

The surface charge formation on the particles was evaluated using particle electrophoresis (Appendix VI). An understanding of surface charge development on particles is important in aqueous processing because it often dictates the tendency of the particles toward agglomeration as well as the type of polymer that may be required to ensure dispersion and flowability of the

suspension. It was found in the current work for hydrothermally synthesized tobermorite that the magnitudes of the zeta potentials were consistent with specific adsorption of Ca^{2+} with the isoelectric point of the tobermorite increasing as a function of Ca^{2+}. IEP for the tobermorite ranged from pH 10.3 in deionized, decarbonated water to pH 11.63 in 10^{-4} M $CaCl_2$(aq).

POWDER PROCESSING, GREEN FORMING, HYDRATION AND CHARACTERIZATION STUDIES

In general, the strength and toughness increased with each processing iteration with mechanical properties significantly better than those for conventionally processed OPC. Large, lenticular cracks present in the gel-cast materials motivate the study on the role of the viscoeleastic properties of the materials.

Processing was first performed using OPC (specifically, OPC-Type I19) because of its availability. The cement was mixed with polyacrylamide by hand and using a high shear mixer (Brabender Co.). Those samples mixed with the shear mixer and pressed had a higher bend strength than the samples which were mixed by hand. The samples extruded with OPC and OPC with an MOD calcium silicate (CDCS 18C) showed the highest strength and toughness values. These excellent properties are the result of filling the interstices of the coarser OPC particles with the finer MOD particles to achieve higher initial densities and improved ultimate mechanical properties. This processing method could not be used on the MOD chemically derived powder alone due to the fineness of the powder and the stiffness of the dough which resulted after shear mixing, characterisitics consistent with the large degree of agglomeration present in the MOD powder.

Table 1 shows the compilation of toughness measurements and crack sizes, where possible, for different processing conditions. Figure 1, summarized earlier, gives some of the properties obtained with selected processing steps. The conclusions from this study are as follows:

1. Samples mixed with a Brabender mixer and without acetone had the highest toughness value (1.4 $MPam^{1/2}$).
2. Samples cured in $Ca(OH)_2$ solution showed the worst mechanical properties. All the flexure beams did not break from the indent because there were large, long cracks (>1000 μm) present. It's not clear if those cracks pre-existed before grinding and drying, or not.
3. In general, the microstructure obtained from the fracture surface showed no substantial difference between processing techniques. Most of the pores are less than 5 μm. However, those cured in $Ca(OH)_2$ solution have a different morphology in the

Table 2. Summary of mechanical properties of OPC paste cured and processed at different conditions

Condition	σ_f(MPa)	K_c(MPa $m^{1/2}$)	Flaw size (μm)
$Ca(OH)_2$ solution	13	---	>1000
" "	21	---	>1000
" "	17	---	>1000
" "	4	---	>1000
" "	10	---	>1000
H_2O solution	19	---	>200
" "	30	0.76	---
" "	26	1.02	---
" "	23	0.94	---
Brabender	55	1.41 (1.19*)	326
" "	59	1.43*	387
" "	40	---	---
" "	44	---	---
Brabender+acetone	19	0.87	---
" "	26	1.25	---

Note:
1. --- means those did not break from indent.
2. * means toughness calculated from fracture surface analysis.
3. Samples were die pressed at 117 MPa and cured at 60°C for 7 days.
4. Beams were indented at 2 and 10 Kgs and fractured in 3-pt. flexure.
5. Compositions are: 7g water + 3g acrylamide + 40g OPC + 0.0154g $(NH_4)_2S_2O_8$
6. $Ca(OH)_2$ solution is prepared 1g $Ca(OH)_2$ in 500 ml water.

outer surface than on the interior. This implies that the infiltration is not as complete as expected or that the green body has no connected pore channels.

4. The long surface cracks may develop because of this infiltrated outer layer since it tends to lose water during the drying period (80°C/17 hours) and there most likely is differential shrinkage at the interface of the surface and interior.
5. Even after use of the high shear, Brabender mixer, there still existed large flaws (cracks) associated with a needle shaped low density region.

GEL-CASTING OF CEMENTIOUS SYSTEMS: MECHANICAL AND VISCOELASTIC PROPERTIES

Gel-casting (Appendices IV, VII, VIII, AND IX) is a forming technique that may be used to potentially develop new cements based on advanced forming techniques, but without the high shear forming required to process the materials when the low water content is reduced to promote higher strength. In gel-casting, water and the monomeric form of the desired polymer are mixed with the ceramic precursor with an appropriate polymerization initiator to form the desired polymer in-situ within the powder mass[3,4]. The rationale for evaluating gel-casting as a cement forming technique was that the liquid, monomeric form of the polymer could be used to replace some of the water used to promote flow in castable cements. After forming and polymerization, the gel-cast polymer would form a rigid three-dimensional structure to promote strength in the mature, cured material.

There were two aspects to the gel-casting work performed in this study. In the initial work (Appendices IV and VIII), the strength of gel-cast cements were evaluated using the critical flaw analysis applied to cementitious systems by Chou et.al. (Appendices I and II). This initial work indicated that the ability to achieve high strength in gel-cast bodies was compromised by lenticular flaws. It was hypothesized that these flaws were due to poor control over the viscoelastic properties of the gel-cast system during the forming process. Therefore a second study was initiated to determine the viscoelastic properties of a model gel-cast system in which non-reactive particles were incorporated (Appendices VIII and IX). Results and conclusions of the processing - property study is described first followed by a discussion of the results obtained on the viscoelastic properties of the model gel-cast system

Processing and properties of gel-cast cementitious systems

There are many variables to take into consideration when gel-casting cement. One such variable is to select the initiator for the polymerization reactions. The experiments showed that there was little difference in strength of gel cast cements whether ammonium persulfate or the

potassium form was used. Another variable evaluated was the method used for mixing the paste. Shear mixing, as opposed to hand mixing, produced cement bars with much higher strengths and denser microstructures. Curing conditions of cement samples also had an effect on the strength. The samples cured in $Ca(OH)_2$ or acetone had much lower strengths than those cured in deionized water. The low strength in the former is attributed to the formation of low strength $Ca(OH)_2$ (Portlandite) platelets. Low strength in the acetone cured cements is attributed to dehydration of the material, in particular the gel-cast polymer. Tanaka showed that polyacrylamide gels shrink via dehydration in the presence of acetone (5). In the current work, curing in acetone was performed to test the hypothesis that some dehydration could put the material into compressive stress and promote greater bend strength. This was not found to be the case as the strength degraded considerably. However, if the appropriate acetone-water mixture is used, there may be improved strength through the formation of only surface compressive stresses.

Processing of the gel-cast cement also played a role in the strength achieved for the final product. Initially the calcium silicate cement powders were uniaxially pressed, but these samples separated when placed in water for curing. The calcium silicate samples were then isostatically pressed to 30,000 psi (107 MPa). These samples did not delaminate during the curing process. However, the strength of the samples were not as high as expected. The microstructure revealed large lenticular cracks, probably due to the uniaxial pressing step. The lenticular cracks were typical of those produced in ceramic materials in which "springback" or the viscoeleastic recovery after applying uniaxial stress to a powder compact exceeds the yield strength of the material. Therefore, work was conducted to examine the viscoelastic response of the gel-cast materials.

Viscoelastic relaxation of gel-cast polyacrylamide containing inorganic filler

The viscoelastic relaxation of gel-cast polyacrylamide was studied as a fucntion of various paprameters including the concentration of cross-linking agent (Appendices VIII and IX). Silica particles were also added to some of the gel-cast polymers and diametral tensile strength determined as a function of the gel-cast polymer processing variables to correlate viscoelastic characteristics of the material to strength. To relate the gel-cast system to cementitious gel cast systems, the influence of inorganic agents (i.e., Ca^{2+} and Na^{+}) that potentially cross-link the polymer were also evaluated. The influence of the different cross-linking agents was determined using isothermal calorimetry to deduce heat production during the reactions, Raman spectroscopy to evaluate molecular structure, and creep-relaxation experiments to determine the viscoelastic behavior of the polymer. Typical viscoelastic responses of the gel-cast polymers as a function of the concentration of organic crosslinking agent are shown in Figure 3.

It was demonstrated that Ca^{2+} and Na^{+} effect the heat production and molecular structure more than any other tested variables and this in turn is reflected in the viscoelastic relaxation of the

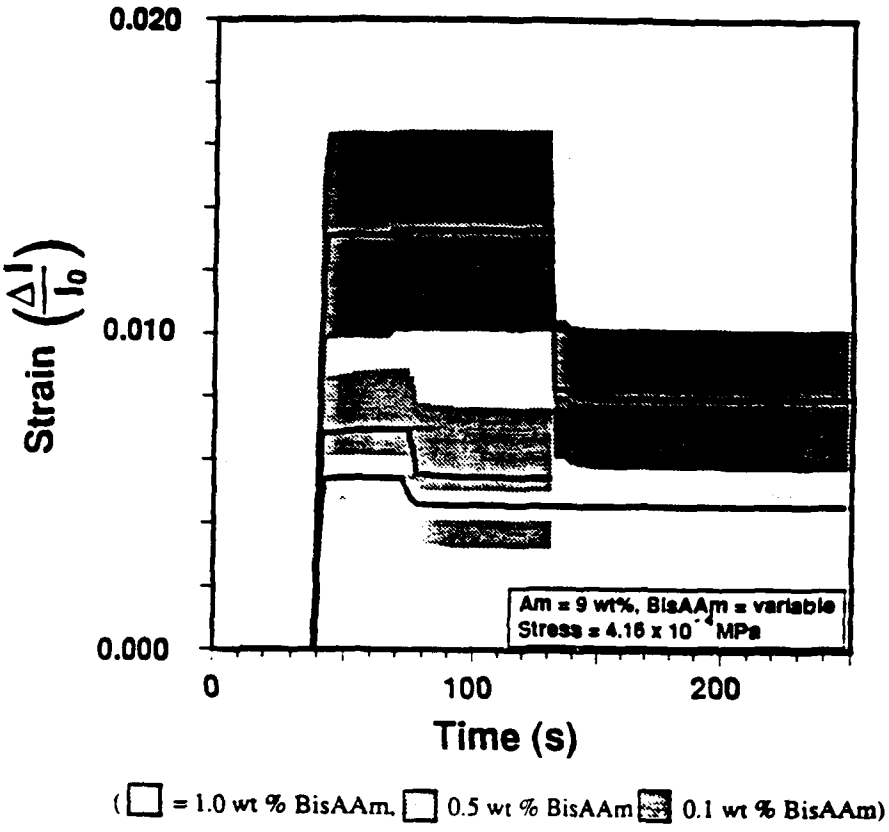

Figure 3. Strain - time diagrams for different polyacrylamide gels. Lines are mean values while shaded regions indicate standard deviation.

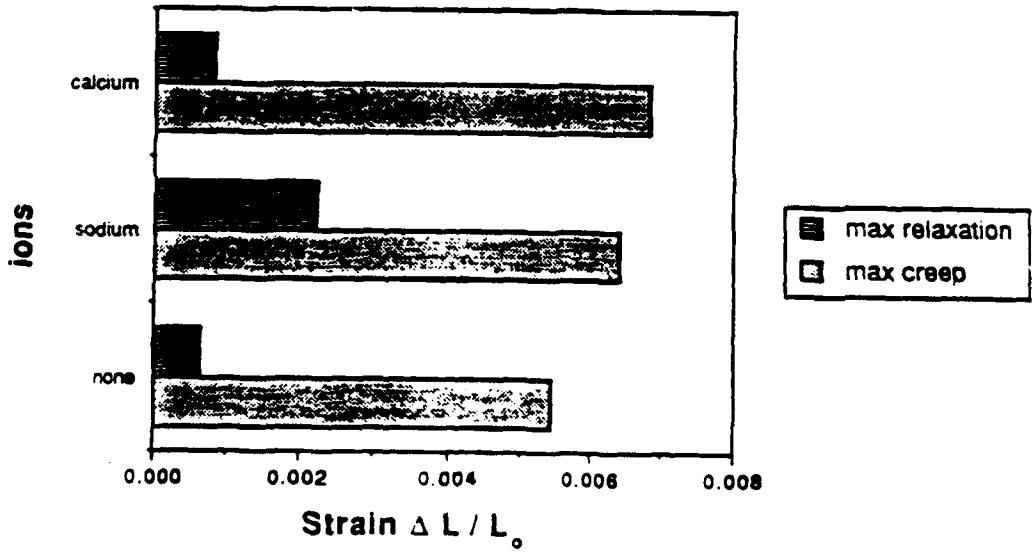

Figure 4. Maximum relaxation and creep for samples with 9 wt% acrylamide and 1 wt% N,N' methylene-bis-acrylamide as the organic cross-linking agent with Ca^{2+} and Na^{2+} present to promote cross-linking via inorganic bonds.

gels after a stress is applied. Na^+ as NaOH had, of course, an explicit impact on the pH of the gel-cast system. It was shown that changes in pH result in differences in molecular structure and viscoelastic relaxation. Gels made with Na^+ are more anelastic because deformation of the formed chain entanglements is permanent. In contrast, samples prepared with Ca^{2+} restore elastically to some extent after stress is applied (Figure 4).

The viscoelastic behavior of gel-cast samples was reflected in the strength of samples with a silica filler present. More elastic samples showed the greatest strength (Table 3). The organic cross-linking agent also produced greater strength than the inorganic. Thus, in general, the viscoelastic behavior of a material during processing has an impact on the subsequent mechanical properties.

CONCLUSIONS

The following conclusions can be drawn from the results of work in this program:

1. The approach using iterative processing combined with fracture mechanics analyses is a powerful tool in the development of high strength cements. Although the mechanical property values reported in the current work do not exceed those reported in the literature, the appreciation developed for magnitudes of the critical flaw sizes as a function of processing mode provide a basis to continue to improve the strength of this important class of compounds.
2. The fracture mechanics approach indicates that bend strengths of 59 MPa and fracture toughness greater than 1 $MPa \cdot m^{1/2}$ can be achieved in ordinary Portland cement without a great deal of changes in the processing. Critical flaw values for these ranges of strength and fracture toughness are ~300μm. This critical flaw size is the same order of magnitude as the biggest particles in the OPC powder before hydration. Thus, greater property improvement may be realized by reducing particles sizes to below at least 100μm.
3. Gel-casting approaches offer a way to improve the ability to process and form advanced cementitious materials without compromising the relatively high strength and fracture toughness values that are being achieved with these materials. Other polymers should be explored and their viscoelastic properties used as a selection criteria to approach optimal mechanical property values in gel-cast cement systems.

Table 3. Overview of the results from the diametral tensile strength testing.

Iteration	sample variables	samples tested	brittle samples	plastic samples	average brittle samples +/-Sd **
	BisAAm in Wt %				
25	0.03	5	5	0	6.46 +/- 0.47
30	0.10	4	4	0	4.33 +/- 0.31
26	0.15	5	5	0	4.56 +/- 0.30
23	0.30	4	4	0	3.57 +/- 0.23
31	0.40	5	5	0	3.01 +/- 0.33
	pH adjusted with Na^+				
27	11.61	4	2	2	3.23 +/-0.065
32	12.65	5	2	3	2.26 +/- 0.21
34	9.38	5	2	3	1.59 +/- 0.32
	pH adjusted with Ca^{2+}				
28	11.46	5	2	3	3.32 +/- 0.06
33	12.21	5	4	1	2.17 +/- 0.21
35	9.63	5	3	2	1.59 +/- 0.28
	grain size in micron				
23	30	4	4	0	3.57 +/- 0.23
36	10	4	4	0	4.65 +/- 0.8
24	5	5	5	0	5.83 +/- 0.75

* BisAAm = N,N - Methelene - bis -Acrylamide

**Average = diametral tensile strength average of the samples in Mpa

REFERENCES

1. Y-S. Chou, J.J. Mecholsky, Jr. and M. Silsbee, "Fracture Toughness of Macro-Defect Free Cement Using Small Crack Techniques." J. Materials Research, Accepted for Publication, 1990.

2. Y. Mai, B. Barakat, B. Cotterell and M. Swain, Proc. Advanced Materials 13, Materials Research Society, Tokyo, Japan (1988).

3. W.M. Kulicke, N. Bose, and M. Bouldin, "The Role of Polymers in Enhanced Oil Recovery," Water Soluble Polymers for Petroleum Recovery, Eds. G.A. Stahl and D.N. Schulz1-17 (1988).

4. Toyoichi Tanaka, "Gels," Scientific American 244, 124-155 (1981).

PAPERS PUBLISHED OR PRESENTED

Y.S. Chou, J.J. Mecholsky, Jr., M.R. Silsbee, D.M. Roy, J.H. Adair, and P.M. Heiland, "Indentation Fracture of Macro-Defect-Free (MDF) Cements" Mat.Res.Soc.Symp. 179, 123-128 (1991) Appendix I

Y.S. Chou, J.J. Mecholsky, Jr., and M.R. Silsbee, "Fracture Toughness of Macro-Defect-Free Cement Using Small Crack Techniques," J. Mater. Res., 5 [8], 1774-1780 (1990). Appendix II

T. Nagira, S.A. Warner, J.J. Mecholsky, and J.H. Adair, "Chemical Processing of Metal Alkoxide Derived Calcium Silicate Chemically Bonded Ceramics," Ibid., Volume 13, Advanced Cements and Chemically Bonded Ceramics, M. Daimon, S. Somiya, G. Sudoh, and K. Takemoto (senior editors), pp.255-262, 1989. Appendix III

S. Venigalla, P.M. Heiland, B.E. Scheetz, and J.H. Adair, Appendix V

P.M. Heiland, J.H. Adair, B.E. Scheetz, Y.-S. Chou, and J.J. Mecholsky, "The Use of Gel-casting in the Fabrication of High Strength Chemically Bonded Ceramics," to be submitted to J. Cement Concrete Res. Appendix VII

K. Maes, M.R. Silsbee, B.E. Scheetz, J.H. Adair, and D.M. Roy, "Gel-Cast Organic-Inorganic Systems," accepted for publication in Proceedings of the Materials Research Society, 1991.

S. Venigalla, P.M. Heiland, B.E. Scheetz, and J.H. Adair, "Crystal Growth Modeling of Hydrothermally Derived Calcium Silicate Hydrates," to be submitted to J. Am. Ceram. Soc.

Theses Defended

Petra M. Heiland, Processing and Properties of Chemically Derived Calcium Silicate Cement, Master of Science, Solid State Science, The Pennsylvania State University, May 1990. Appendix IV

Kelly Markowski, A Fundamental Study of the Surface Chemistry of Calcium Silicate Hydrate, Bachelor of Science Thesis, Ceramic Science and Engineering, The Pennsylvania State University, May, 1990. Appendix VI

Kathleen Maes, Characterization and Use in Gel Casting Ssytems of Different Polyacrylamide Admixtures, Master of Science, Solid State Science, The Pennsylvania State University, defended August, 1991, approval by gradute school pending.

PERSONNEL

The Pennsylvania State University

B.E. Scheetz	Associate Professor, Solid State Science
M.R Silsbee*	Postdoctoral Research Associate
P.M. Heiland	Graduate Assitant, Solid State Science
Yeong-Shyung Chou	Graduate Assistant, Ceramic Science and Engineering
K. Maes	Graduate Assitant, Solid State Science
K. Markowski	Senior in Ceramic Science and Engineering
S. Hastings	Senior in Ceramic Science and Engineering

University of Florida

John J. Mecholsky, Jr.	Professor, Materials Science and Engineering
James H. Adair	Assoicate Professor, Materials Science and Engineering
F. Jeffrey Opalko	Senior Chemist, Materials Science and Engineering
John Niaouris	Graduate Associate, Materials Science and Engineering
Sridhar Venigalla	Graduate Associate, Materials Science and Engineering

---

*Dr. Silsbee did not receive salary compensation from this contract. Work was completed in conjunction with contract MSS-8718111.

APPENDIX I

Y.S. Chou, J.J. Mecholsky, Jr., and M.R. Silsbee, "Fracture Toughness of Macro-Defect-Free Cement Using Small Crack Techniques," J. Mater. Res., 5 [8], 1774-1780 (1990).

Fracture toughness of macro-defect-free cement using small crack techniques

Y-S. Chou, J. J. Mecholsky, Jr.,[a] and M. Silsbee
The Pennsylvania State University, University Park, Pennsylvania 16802

(Received 21 November 1989; accepted 12 April 1990)

The fracture toughness of a macro-defect-free (MDF) cement was calculated from two measurement techniques: (1) indentation-strength method and (2) fracture surface analysis (FSA). It was found that the indentation-strength method, which showed good agreement with FSA, was applicable for estimating the fracture toughness of MDF cement. The ultimate toughness was found to be 1.25 MPa $m^{1/2}$ for this MDF cement, which contained 3 wt.% polymer. An R-curve (crack-growth-resistance) behavior was also observed. Scanning electron micrographs showed extensive microcracking on the fracture surface. Microstructural effects are discussed.

I. INTRODUCTION

Cement is an inexpensive, readily available material with many desirable properties. Nevertheless, it is rather weak in structural applications compared with traditional ceramics such as alumina and zirconia. The fracture toughness (K_k) of conventional hydrated cement paste varies from 0.2–0.5 MPa $m^{1/2}$,[1-3] which is rather poor compared to other ceramics; e.g., alumina has K_k values which range from 2–6 MPa $m^{1/2}$. The low toughness and large flaws lead to very low flexural strength, typically between 3 and 10 MPa.[4] It has been demonstrated that porosity is by far the dominant controlling factor limiting the strength of hydrated cement paste.[5-7] The removal of those large voids, i.e., macro-defects, by using polymers and plasticizers for rheological control and efficient mixing has generated a new class of materials: MDF (macro-defect-free) cements. Investigators have shown that the flexural strength of MDF cements then increases to 70 MPa and fracture toughness can reach 3.0 MPa $m^{1/2}$.[8]

The measurement of fracture toughness of cement paste has been conducted mostly using the single-edge-notch-beam (SENB) method on ordinary portland cement[2,3,7,9] and alumina cement.[10] Some researchers used the double-cantilever-beam (DCB) technique on cement paste, mortars,[11] and concrete,[12] and double torsion (DT) to study the crack growth in hardened cement paste.[13] There are many papers discussing the measurement of toughness of MDF cement. Eden and Bailey used the SENB technique and work of fracture to calculate K_k and proposed a fibrillar pull-out model for polymer modified portland cement.[14] Mai *et al.*[15] attempted to use indentation cracks and large cracks in double cantilever beam (DCB) specimens to measure crack resistance but succeeded only with the DCB technique. None of them employed the indentation-strength technique.[16] This technique is attractive because it involves crack sizes observed in most advanced materials applications. Since there appears to be a crack size effect on fracture resistance, it is important to know the behavior, i.e., strength and toughness, for small cracks as well as large cracks. Typically, small cracks control the strength of the material. Fracture surface analysis (FSA), which has been proven very powerful in glass and ceramics, is used to determine the fracture toughness of MDF cements. It is our goal in this paper to investigate the applicability of the indentation method and FSA to MDF cements.

II. EXPERIMENTAL

MDF cement was prepared by mixing 83 parts (by weight) of ordinary portland cement (a calcium silicate based material), 14 parts of de-ionized water, and 3 parts of polymer (polyacrylamide). For better processing, the polymer was first dissolved in water, then mixed with cement particles. After shear mixing, the paste was extruded into a plate and cured at 60 °C in a humid atmosphere for one week. The relative humidity was kept around 90%. The extruded plate was sandwiched by two flat glass plates with a dead weight (about 4 Kgs) to prevent warping during this curing period. The plate was then placed at ambient temperature and atmospheric condition for another 3 weeks and cut into rectangular beams (approximately 5 × 3 × 40 mm). To remove existing surface flaws or those resulting from cutting, all beams were ground using 600 grit and dry polished with 1 μm alumina powder. To avoid stress concentrations at sharp edges, all beam corners were rounded. During each grinding/polishing step, beams were cleaned with ultrasonic vibration for 5–10 min in acetone. Finally, they were coated with gold.

[a]Current address: University of Florida, Department of Materials Science and Engineering, Gainesville, Florida 32611

After coating, beams were indented by a Vickers diamond using loads from 1 Kg to 15 Kg and fractured in 3-pt flexure (outer span = 25.4 mm). The crosshead speed was 2.54 mm/min. After fracture, samples were immediately coated with gold to prevent possible hydration. An uncoated fracture surface was observed after exposure to air for an extended time; the surface was altered in such a way as to change the morphological details. Although the hydration of cement usually depends on the original water in the mix, the water/cement ratio in the present mixture is low (0.17) and the original water is most likely completely reacted. In fact, there was evidence of unreacted calcium silicate particles (cf. Fig. 2) which could react with external water; thus, the samples were coated. The coated specimens were analyzed using optical and electron microscopy. Fracture surfaces were first evaluated using a stereoscope (Nikkon) with magnification from 6.6 to 40×. Fracture markings such as "river" markings, lance, and twist hackle were helpful in tracing the fracture path back to the origin.[17] These markings have been observed on glasses, single and polycrystal ceramics, metals, and polymers.[17] In addition, the amount of polymer used in these experiments was about 3 wt.% and most likely did not form a continuous network or precipitate as a particle. Thus, we expect brittle-like behavior with the associated features, as observed. Fracture surfaces were also examined on a scanning electron microscope where the depth of field was utilized. Both secondary and backscattered electron images were used to delineate the markings.

In general, it is very difficult to observe fracture features in cementitious material. In order to attempt to produce a more visible fracture origin, we decorated the indented crack surface. To decorate the origin, two extra flexure beams were indented and marked with a drop of liquid of either (1) mixture of 5:1 = absolute ethanol:black ink or (2) 10 drops of concentrated nitric acid in 50 ml absolute ethanol at the impression. They were then broken and analyzed as the others.

III. BACKGROUND

There are two popular methods used to obtain fracture toughness using indentation: (1) the direct crack measurement and (2) the strength method. The former involves indentation and measurement of the crack surface trace length. This measurement provides a quick estimation of the resistance to fracture, but the crack propagation process is not considered since the toughness is estimated from the length of the arrested crack. This suggests that perhaps the arrested indented cracks should be associated with the stress intensity for crack arrest, K_a, rather than K_c, the critical stress intensity for catastrophic failure.[18] Also, the surface for the direct-indentation method should be as flat as possible and free from flaws, a condition which is almost impossible for cement paste. These considerations directed us to choose the indentation-strength method for evaluation of fracture toughness.

Consider a Vickers-induced radial crack system, subjected to an applied tensile stress σ_a, as depicted in Fig. 1. The stress intensity factor, K_a, appropriate to this tensile loading has the standard form

$$K_a = Y\sigma_a c^{1/2} \tag{1}$$

where Y is a load and crack-geometry factor ($Y = 1.24$ for small surface cracks which are residual-stress free) and c is the critical crack size where $c = (ab)^{1/2}$ with a = depth and $2b$ = width of the fracture initiating crack.[19] For the Vickers crack system, the crack extension force comes from not only the applied load but the deformed region which gives the residual stress. The stress intensity factor for the residual part is

$$K_r = \chi_r P/c^{3/2} = y_v(E/H)^{1/2}P/c^{3/2} \tag{2}$$

where χ_r and y_v are constants for the Vickers-produced radial crack and E/H is the elastic modulus-to-microhardness ratio.[20] The net stress intensity factor is therefore

$$K_t = K_r + K_a = \chi_r P/c^{3/2} + Y\sigma_a c^{1/2} (c > c_0') \tag{3}$$

where c_0' is the size of the radial crack immediately prior to application of the tensile stress.[16] For crack growth under equilibrium conditions, $K_t = K_c$, we can solve the applied stress as a function of crack size,

$$\sigma_a = [K_c/Y_c^{1/2}][1 - \chi_r P/K_c c^{3/2}] \tag{4}$$

This equation has a maximum at $d\sigma_a/dc = 0$, which gives the fracture strength, σ_m, and the maximum crack size, c_m, beyond which the crack propagates unstably to catastrophic failure.

$$\sigma_m = 3K_c/4Y(c_m)^{1/2} \tag{5}$$

$$c_m = (4\chi_r P/K_c)^{2/3} \tag{6}$$

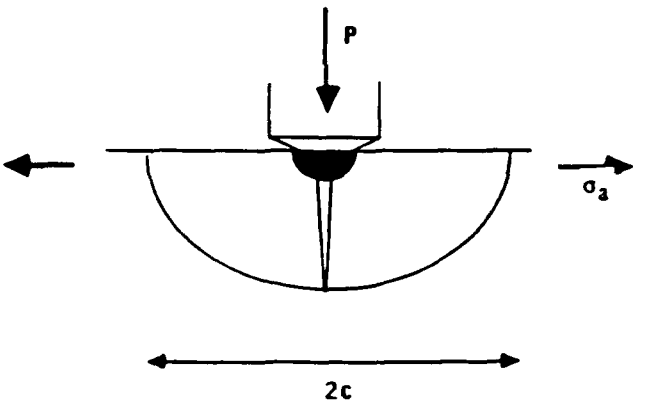

FIG. 1. Schematic of Vickers-produced radial/median crack system, characteristic crack dimension, c, with contribution to tensile loading and residual stress field (via central deformed region) at (preceding) contact load P.[14]

Chantikul *et al.*[3] derived an expression for toughness from Eqs. (5), (6), and (2),

$$K_c = \eta(E/H)^{1/2}(\sigma_m P^{1/3})^{3/4} \quad (7)$$

where η is another geometrical constant ($\eta = 0.59$). Note that K_c is used here because the crack introduced during indentation is a stable crack and may be different from K_{Ic}. However, in practice the values are often close.

In order to determine the fracture toughness from a measurement on the fracture surface of the size of the indented crack for bars which contain local residual stress due to the indentation process, we can rearrange Eq. (5) and substitute $Y = 1.24$ and obtain[3]:

$$K_c = 1.65\sigma_f c^{1/2} \quad (8)$$

Fractography is a powerful tool in fracture analysis. Not only can we find the fracture origin but also we can calculate either the toughness or strength using this technique. The identification of fracture origins such as pores, agglomerates, or contact damage can provide valuable information for process control. The critical flaw size can also be used to estimate fracture strength. In reality, ceramic parts with known toughness fail during service, often without knowing the fracture strength. Fracture strength can be calculated using either Eq. (1) or Eq. (8) when toughness and critical flaw sizes are known to provide important information on the stress distribution.

IV. RESULTS AND DISCUSSION

A. Fracture surface analysis

Samples were first examined with a stereoscope using oblique lighting[21]; this technique is essential for tracing fracture features back to the origin. One of the advantages for using the indentation technique is that the indent, most of the time, serves as the flaw, unless large defects or unrounded corners causing stress concentrations also exist.) Even though the traces of the indent cracks were not clear, as observed by Mai *et al.*[3] as well, the origin of failure occurred at the indentation site and was from a typical indentation crack (i.e., the average depth to half-width ratio was approximately 0.8–1.0. One technique to locate the critical flaw is to examine fracture markings on large grains at high magnification. A typical example of the fracture surface of an unreacted cement particle is depicted in Fig. 2. Twist hackle markings are clearly distinguishable and point downward to the origin—in this case, the indent.

Once we optically identify the flaw origin, we examine the surface to measure the flaw size using scanning electron microscopy. Two different images were taken, i.e., the secondary and backscattered electron images. Surface charging due to edge effects and localized roughening are present when using the secondary

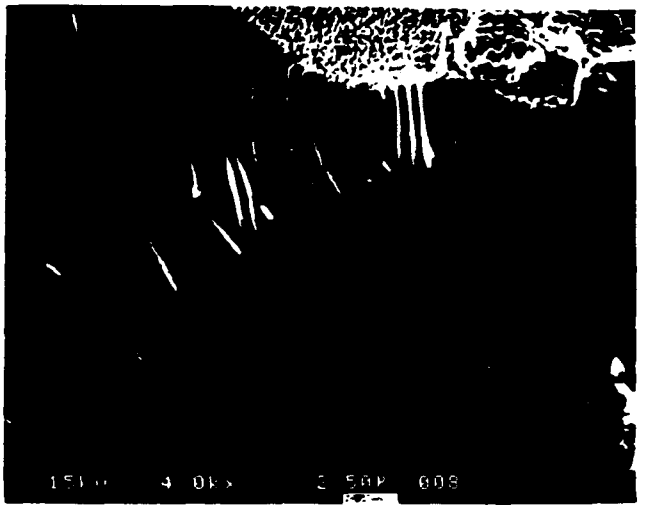

FIG. 2. A typical example of locating the failure origin by examining the fracture surface of an unreacted large cement particle at high magnification. The twist hackle points back toward lower right) to the origin.

electron images. These problems can be eliminated by using the backscattered electron image shown in Fig. 3 and as successfully demonstrated by Healey and Mecholsky.[22,23] It can also be seen that the backscattered image illuminates the fracture markings better than the secondary image. Note that Healey and Mecholsky[22] used a four-quadrant solid-state annular backscattered detector which provides an enhanced topographical image.

B. Fracture toughness of MDF cement

The fracture toughness of MDF cement calculated by the indentation-strength method, Eq. (7), and fracture surface analysis, Eq. (8), is listed in Table I. The toughness versus flaw size is shown in Fig. 4. These two different methods show good agreement. The apparent toughness value is taken at the asymptote value to be 1.25 MPa m$^{1/2}$. The word "apparent" used here means that though the two methods show good consistency, it does not necessarily mean that the asymptote value is the true or ultimate toughness value.[24] It has been known that a number of factors could affect the fracture toughness of MDF cements, such as porosity, water-to-cement ratio (W/C), type of cement and polymer, volume fraction of polymer and curing condition, etc. Eden and Bailey[4] used ordinary portland cement with W/C = 0.13–0.17, 1–4% polymer, and cured in water for 7 days. The toughness values for their studies increased from 0.7 to 1.0 MPa m$^{1/2}$ with increased polymer fraction from 1.5–5%, respectively. Alford *et al.*[5] also obtained toughness values from 0.71 to 1.04 MPa m$^{1/2}$ using OPC and polyacrylamide, cured at 100% R.H. (30 °C) for 7 days, then dried at 50% R.H. for another 7 days.[5] As for alumina cement, toughness val-

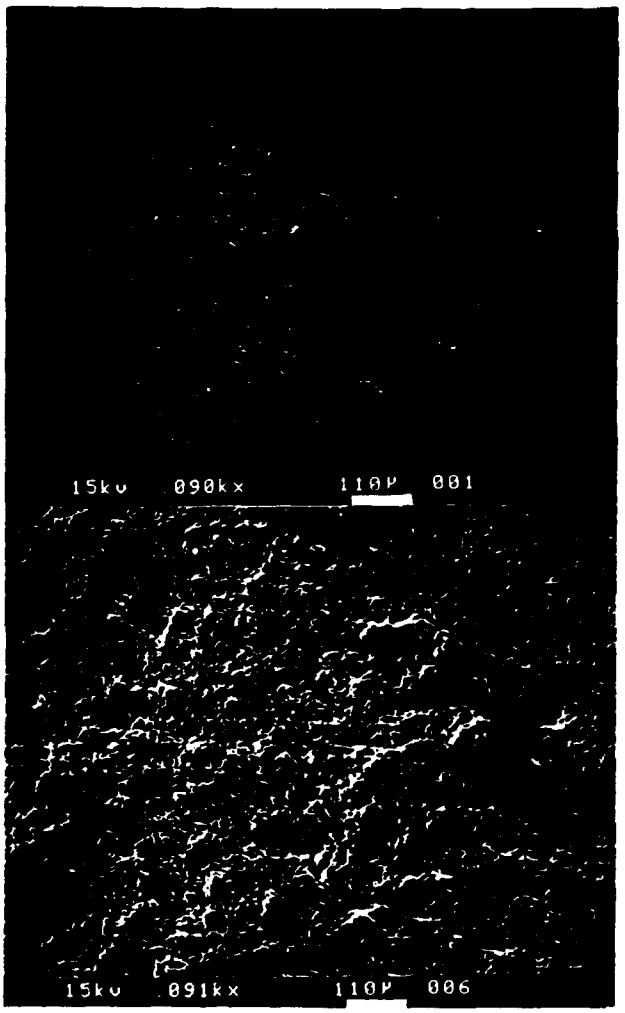

FIG. 3. Fracture surface images showed no surface charging taken by backscattered electron image (above) rather than the secondary electron image (below).

ues as high as 3.1 MPa $m^{1/2}$ have been reported.[8] Our toughness data are higher than those of typical OPCs, most likely due to the higher curing temperature (60 °C). The curing temperature of 60 °C was chosen based on our previous unpublished work, which showed that paste cured at 60 °C in water for 1 week produced higher toughness than that cured at 30 °C. The reason for this difference may be that the higher temperature speeds up the hydration process and softens the polymer (60 °C is higher than the glass transition temperature of the polymer used), which can lead to a more uniform microstructure. However, our values are slightly higher than other MDF cements (e.g., Eden and Bailey[14]) with as low a polymer content (3 wt.%) and water-to-cement ratio (0.17). Improvements to these cements are expected if a higher polymer content is added. The maximum limit appears to be about 3.1 MPa $m^{1/2}$.

TABLE I. Test data of MDF cement.

#	Load (Kg)	$K_c(1)$ (MPa $m^{1/2}$)	$K_c(2)$ (MPa $m^{1/2}$)	c (μm)	σ (MPa)
1	1	1.00	1.08	119	59
2	3	1.14	1.12	200	48
3	3	0.95	···	···	38
4	5	1.13	1.1[illegible]	305	41
5	5	1.20	1.11	234	44
6	7	1.24	1.04	237	41
7	7	1.28	1.29	329	43
8	10	1.35	1.25	341	41
9	10	1.28	1.36	497	38
10	15	1.35	1.32	498	36

··· = flaw was not identified, c = flaw size, σ = flexure strength. $K_c(1)$ is calculated from Eq. (7) (indentation). $K_c(2)$ is calculated from Eq. (8) (FSA). Flaw size $c = (ab)^{1/2}$, where a is the depth of the semi-elliptical flaw and $2b$ is the width of the flaw on the surface.

Rice and co-workers found that for ceramics the fracture energy depends on the flaw-size-to-grain-size ratio.[25] They observed that flaw sizes less than 1/2 to 1/4 of grain size cannot be arrested at the grain boundary, and single crystal fracture energy governs fracture resistance below this limit. For flaw-size-to-grain-size ratios of 1 to 6, polycrystalline fracture energy applies. For concrete and mortar, the microstructure is quite inhomogeneous and contains large sand and gravel particles in the centimeter size range. Thus, measurement of toughness using small flaws in-

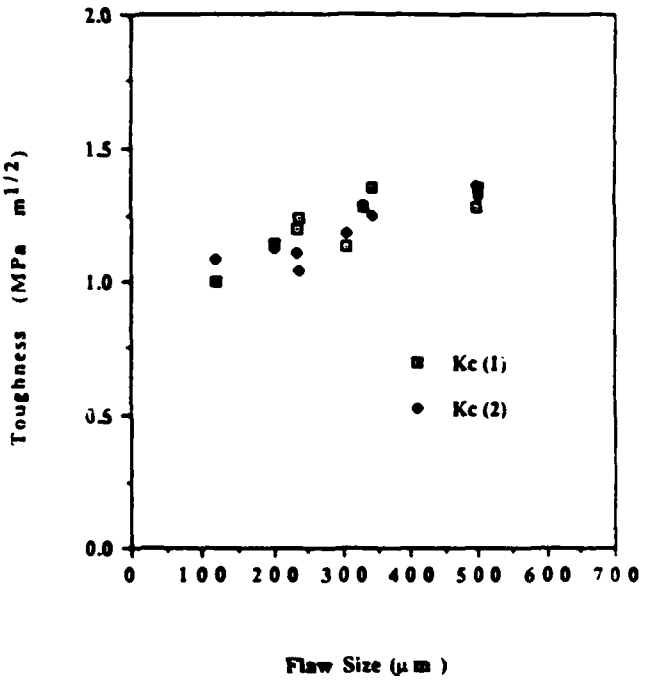

FIG. 4. Comparison of fracture toughness calculated by Eq. (7) and Eq. (8).

troduced by indentation is inappropriate and a notched beam technique is most frequently used. The notch depth is in the same range as the size of sand and gravel,[26] whereas in our MDF cement system, the microstructure composed of unreacted cement particle and hydrated product showed grain sizes less than 50 μm, as in Fig. 3 (which is quite obvious since the initial particle size of cement is in the 10–20 μm range). The flaws introduced by the indentation technique lie in the range of 100–500 μm, which are small compared with conventional test methods such as the double cantilever beam, double torsion, or notched beam techniques[11,13]; however, they are quite large compared to the microstructure. In Fig. 5 we plot the flexural strength versus indent load in logarithmic coordinates. If we assume that Eq. (7) can be applied to MDF cements, then strength values at higher indent loads should approach a line with slope of $-1/3$. Most polycrystalline ceramics deviate from this ideal behavior at lower indent loads because of a decrease in toughness with decreasing crack sizes. For our cement, at high indent loads the strength values are consistent with an approach to an ideal $-1/3$ power dependence on indent load, as suggested by Eq. (7), indicative of a nonvarying toughness. However, in order to justify this assumption and determine whether this is truly a toughness-crack size plateau, more data at higher indent loads are needed. Because the thicknesses of our beam samples were limited to about 3 mm due to processing and were rather thin, the highest indent load was therefore limited to about 15 Kgs. Further investigation on the $-1/3$ slope at much higher loads is still needed when thicker samples are available. The deviation from the $-1/3$ slope curve at low indent loads is consistent with other ceramic materials.[24,27] This behavior leads to a nonconstant toughness.

Crack extension resistance (toughness) increases with the flaw size, a so-called R-curve behavior (Fig. 6). It has been interpreted by Cook[24] that at small flaw sizes, i.e., comparable to the scale of the microstructure, the toughness is an intrinsic property representing the weakest fracture path, and at larger flaw sizes the toughness reaches a steady-state value representative of the cumulative crack/microstructure interactions in polycrystalline materials. For our MDF cements, the R-curve is somewhat flat (Fig. 6). We do not know yet whether this flat R-curve is due to its intrinsic properties or that we just haven't used a load low enough to create flaw sizes smaller than 100 μm. The lower indentation range seems impossible to achieve at present since the intrinsic flaws in our cement samples are in the 100 μm range.

Cook and Clarke have proposed a power law dependence for the fracture resistance, and hence toughness, on crack length[27]

$$T = T_0(c/d)^{\tau} \qquad (c >= d) \tag{9}$$

where T is toughness, T_0 is the base line toughness of the material in the absence of any toughening mechanisms, and the scaling term d is the spatial extent of the crack at which toughening begins. The toughening exponent τ characterizes the rate at which the toughness increases ($\tau = 0$ corresponds to constant toughness, for

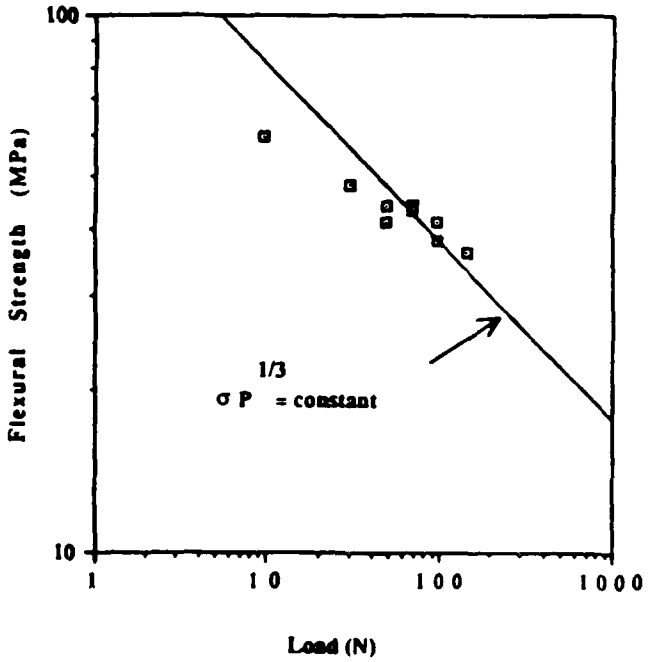

FIG. 5. Flexural strength versus indent load is consistent with a $-1/3$ slope at high indent loads.

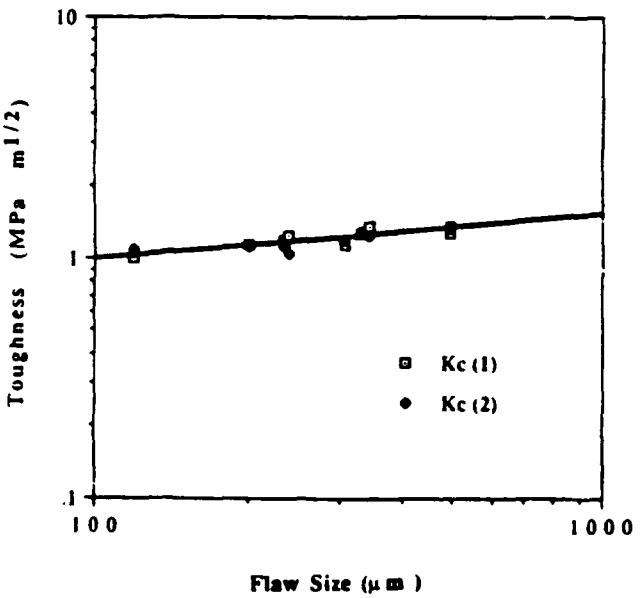

FIG. 6. Toughness versus crack size relationship fits a power law expression [Eq. (9)].

R-curve behavior $\tau > 0$). For MDF cements this model will have to be carefully tested to see if it applies. The testing of this model is beyond the scope of this paper.

A fibrillar pull-out model has been proposed by Eden and Bailey[14] for high strength polymer modified portland cement. From observations of the fracture surface in Fig. 7, we found no indication of fibrillar pull-out. Crack bridging due to localized grain bridging, polymer fibril bridging, and/or frictional interlocking behind the crack front was suggested by Mai *et al.*[15] as a mechanism for toughening in a calcium aluminate MDF cement. We had a different starting material and a different polymer, both of which influence the microstructure and properties. We saw no evidence of the crack bridging phenomenon. However, microcracking was observed not only directly beneath the indent, but also approximately evenly distributed throughout the whole specimen. The toughening mechanism is attributed to this microcracking. Since microcracking can occur from drying in a vacuum and from electron beam heating,[28] a polished sample from the same batch was examined in the SEM and was observed to have no microcracks due to drying or electron beam heating. Traditionally, the word "microcracking" was used in polycrystalline ceramics such as lead titanate or partially stabilized zirconia, which showed cracks approximately the size of the grains. However, the microcracking observed in these MDF cements is quite extensive, i.e., of the order of 10–20 μm. We expect that microcracking forms a zone around the crack tip and reduces the near tip stresses.

C. Effect of crack decoration on fracture

Two solutions (ink and acid) were applied to determine if any enhanced visualization could be achieved by decoration. A drop of liquid was placed at the indent on one of the two beams. The fracture surface showed a much clearer contrast for acidic etchant rather than the ink-alcohol solution, as shown in Fig. 8. The toughness for nitric-alcohol is $K_c(1) = 1.41$ MPa $m^{1/2}$ [$K_c(2) = 1.52$ MPa $m^{1/2}$] higher than ink-alcohol $K_c(1) = 1.3$ MPa $m^{1/2}$ [$K_c(2) = 1.23$ MPa $m^{1/2}$], where $K_c(1)$ was calculated using Eq. (7) and $K_c(2)$ using Eq. (8). There are some uncertainties about the effects of the etchant since it may react with the cement paste and cause crack blunting. Thus the higher toughness treated with nitric acid might be due to crack blunting. In addition, the crack which had been made more clear due to the etchant may undergo stable subcritical crack growth before reaching the critical size a_i which the crack propagates to failure.[16] This growth will lead to an underestimation of toughness by FSA techniques [Eq. (8)], since the flaws we observed are those en-

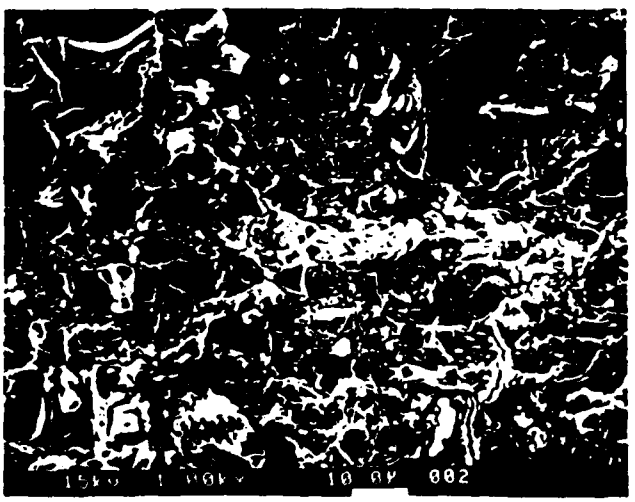

FIG. 7. Fracture surface of MDF cement shows evidence of microcracking.

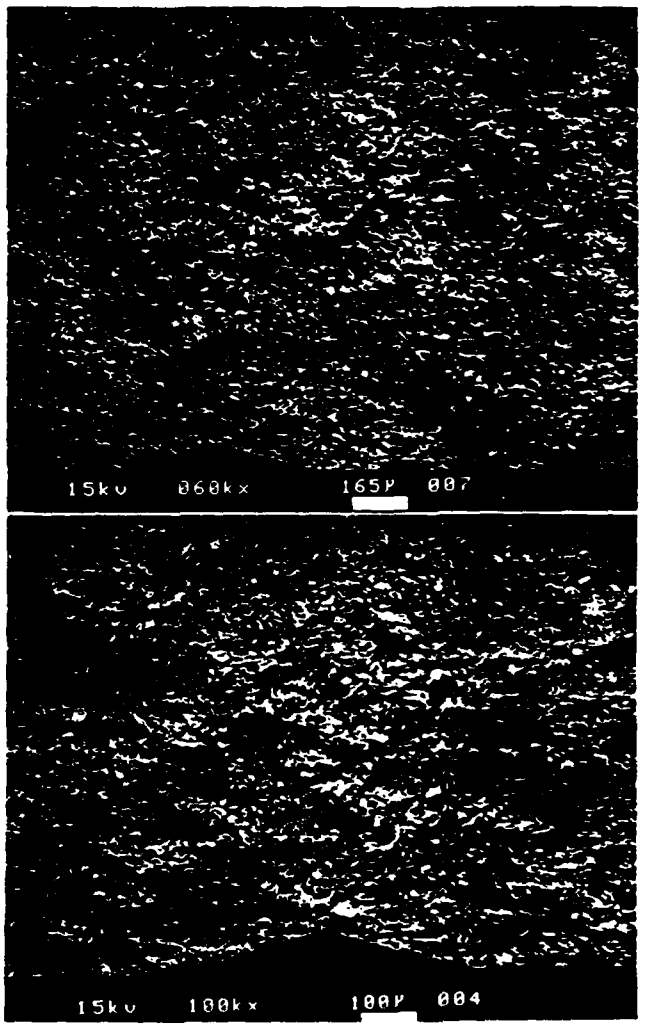

FIG. 8. Fracture surface of samples for which a liquid was placed at the indent; (above): nitric acid-alcohol solution; (below): ink-alcohol solution.

hanced by etchant. However, the data calculated by the indentation-strength and FSA methods turned out to be in good agreement, which implies that the residual stress contribution is rather small compared with the applied stress. Whether this low residual stress is due to the relaxation process of the polymer or to the reaction of the etchant needs further investigation.

V. CONCLUSION

The indentation-strength technique and fracture surface analysis were found applicable to MDF cements for measuring fracture toughness. By using both optical and electron microscopes, fractography becomes a powerful tool to estimate the toughness. Therefore we suggest that small crack techniques are applicable for the measurement of crack growth resistance in cementitious materials as long as the crack size is larger than a characteristic dimension of the microstructure. R-curve (crack-growth-resistance dependence on crack size) behavior was observed and the apparent (ultimate) toughness was about 1.25 MPa $m^{1/2}$. Microcracking was suggested as a possible toughening mechanism for this MDF cement. Current processing techniques limit the study of the fracture process and toughening mechanisms.

ACKNOWLEDGMENTS

This work was supported by the Air Force Office of Scientific Research under Contract No. AFOSR-88-0184; technical monitor was Dr. Liselotte J. Schioler. The authors also wish to acknowledge the useful discussions they have had with Dr. J. Adair and Ms. P. Heiland.

REFERENCES

[1]S. Diamond, in *Very High Strength Cement-Based Materials (Proc. Mater. Res. Soc. Symp.)*, edited by J. F. Young (Materials Research Society, Pittsburgh, PA), Vol. 42, pp. 233–243.
[2]N. McN. Alford, G.W. Groves, and D. D. Double, Cement and Concrete Research 12, 349 (1982).
[3]D. D. Higgins and J. E. Bailey, J. Mater. Sci. 11, 1995 (1976).
[4]J. D. Birchall, A. J. Howard, and K. Kendall, Nature 289, 388 (1981).
[5]D. M. Roy and G. R. Gouda, Cement and Concrete Research 5, 153 (1975).
[6]K. Kendall, A. J. Howard, and J. D. Birchall, Philos. Trans. R. Soc. London A310, 139 (1983).
[7]N. B. Eden and J. E. Bailey, J. Mater. Sci. 10, 150 (1984).
[8]N. McN. Alford and J. D. Birchall, in *Very High Strength Cement-Based Materials (Proc. Mater. Res. Soc. Symp.)*, edited by J. F. Young (Materials Research Society, Pittsburgh, PA), Vol. 42, pp. 265–276.
[9]J. J. Beaudoin, Cement and Concrete Research 13, 81 (1983).
[10]J. J. Beaudoin, Cement and Concrete Research 12, 289 (1982).
[11]J. H. Brown and C. D. Pomeroy, Cement and Concrete Research 3, 475 (1973).
[12]P. Rossi, C. Boulay, P. Acker, and Y. Malier, in *Cement-Based Composites: Strain-Rate Effects on Fracture (Proc. Mater. Res. Soc. Symp.)*, edited by S. Mindess and S. P. Shah (Materials Research Society, Pittsburgh, PA, 1986), Vol. 64, pp. 39–46.
[13]K. D. Bladie and P. L. Pratt, *ibid.*, pp. 47–61.
[14]N. B. Eden and J. E. Bailey, J. Mater. Sci. 19, 2677 (1984).
[15]Y. Mai, B. Barakat, B. Cotterell, and M. Swain, *Proc. Advanced Materials*, Materials Research Society, Tokyo, Japan, 13 (1988).
[16]P. Chantikul, G. R. Anstis, B. R. Lawn, and D. B. Marshall, *ibid.*, 64, 539 (1981).
[17]R.W. Rice, in *Fractography of Glasses and Ceramics*, Adv. Ceram., edited by J. R. Varver and V. D. Frechette, 22, 3–56 (1986).
[18]Z. Li, A. Ghosh, S. Kobayashi, and R.C. Bradt, J. Am. Ceram Soc. 72, 904 (1989).
[19]P. N. Randall, in *Plane Strain Toughness Testing of High Strength Metallic Materials*; edited by W. F. Brown, Jr. and J. E. Srawley, ASTM STP 410, 88–126 (1966).
[20]D. B. Marshall, T. Noma, and A. G. Evans, J. Am. Ceram. Soc. 65, c175–c176 (1982).
[21]R. F. Cook and B. R. Lawn, J. Am. Ceram. Soc. 66, c-200–c-201 (1983).
[22]J.T. Healey and J. J. Mecholsky, Scanning 4, 62 (1981).
[23]J.T. Healey and J. J. Mecholsky, in *Fractography of Ceramics and Metals Failures*, edited by J. J. Mecholsky, Jr. and S. R. Powell, Jr., ASTM STP 827, 157–181 (1984).
[24]R. F. Cook, J. Mater. Res. 2, 345 (1987).
[25]R.W. Rice, S.W. Freiman, and J. J. Mecholsky, Jr., J. Am. Ceram Soc. 63, 129 (1980).
[26]S. P. Shah and F. J. McGarry, J. of the Engineering Mechanics Division, Proc. of the American Society of Civil Engineers (Dec. 1971), pp. 1663–1676.
[27]R. F. Cook and D. R. Clarke, Acta Metall. 36, 555 (1988).
[28]L. Struble, P. Stutzman, and E. R. Fuller, Jr., J. Am. Ceram. Soc. 72, 2295 (1989).

APPENDIX II

Y.S. Chou, J.J. Mecholsky, Jr., M.R. Silsbee, D.M. Roy, J.H. Adair, and P.M. Heiland, "Indentation Fracture of Macro-Defect-Free (MDF) Cements" Mat.Res.Soc.Symp. 179, 123-128 (1991)

INDENTATION FRACTURE OF MACRO-DEFECT-FREE (MDF) CEMENTS

YEONG-SHYUNG CHOU, J. J. MECHOLSKY, JR., M. R. SILSBEE, D.M. ROY, J. H. ADAIR, AND P. HEILAND
The Pennsylvania State University, University Park, PA 16802

ABSTRACT

The fracture toughness of MDF (macro-defect-free) cement with different polymer contents has been investigated by the indentation-strength method and fracture surface analysis. It was found that the fracture toughness obtained by these two different techniques showed good agreement for the low (3 wt.%) polymer cement. The ultimate (apparent) toughnesses are 1.3 MPa $m^{1/2}$ for low polymer content and 2.2 MPa $m^{1/2}$ for high (8 wt.%) polymer content cement. Different microcracking and sponge-like microstructures have been observed and discussed.

INTRODUCTION

Toughness is a measure of the resistance to rapid crack growth and can be measured by either the critical stress intensity factor, K_{IC}, fracture energy, γ_e, or critical strain energy release rate, G_c ($G_c = 2\gamma_e$). These properties can be shown to be interrelated. The measurement of toughness in cements, concrete, and other chemically bonded ceramics (CBCs) has been discussed extensively[1] in the literature. Much discussion in the literature involves the effect of crack size on the measurement of toughness and the mechanisms leading to this phenomenon. If there is a mechanism by which the value of the toughness increases with crack size, then this does not necessarily invalidate a particular test but rather indicates a multi-valued property. These latter materials have been termed "R-curve" materials, where the "R" stands for resistance. Most investigators in cementitious materials have not examined the microstructure along with their mechanical property measurements in order to try and understand the behavior.

Strength alone will not provide sufficient information to determine mechanical behavior. Since strength is dependent on crack size, it can vary with the handling procedure, finishing procedure, or with random processing flaws. Various strength tests are used in the cements literature. These include the diametral compression test,[2] the flexural beam,[3] and the tensile specimen.[4] In most of these tests, the crack or flaw size at the fracture origin is not controlled or measured. Thus, the results of these tests are subjected to statistical scatter, due to the distribution of crack sizes. In this paper we determine the applicability of the controlled (indentation) flaw test for MDF cements so that different processing conditions can be compared for the same indentation conditions.

Mat. Res. Soc. Symp. Proc. Vol. 179. © 1991 Materials Research Society

EXPERIMENTAL

Two batches of MDF cement were prepared by shear mixing, followed by extrusion. Their compositions are listed in Table 1. After extrusion, the plates were cured at 60°C in a humid (R.H. = 90%) atmosphere for one week. The plate was then placed at ambient temperature and atmospheric condition for another 3 weeks and then cut into rectangular beams (approximately 5 x 3 x 40 mm). To remove existing surface flaws or stress concentrations at corners, all beams were carefully ground and polished with 1 μm alumina powder. They were then coated with gold and indented by a Vickers diamond, using loads from 1 Kg to 15 Kg and broken in 3-pt flexure (outer span = 25.4 mm). The cross head speed was 2.54 mm/min. After fracture, samples were immediately coated with gold to prevent possible hydration and analyzed with optical and electron microscopes. Fracture surfaces were examined on optical and electron microscopes.

INDENTATION AND FRACTURE SURFACE ANALYSIS TECHNIQUES

There are two popular methods used to obtain fracture toughness using indentation: (1) the direct crack measurement[15] and (2) the strength method.[16] The former involves indentation and measurement of the crack surface trace length. This measurement provides a quick estimation of the resistance to fracture, but the crack propagation process is not considered, since the toughness is estimated from the length of the arrested crack. This suggests that perhaps the arrested indented cracks should be associated with the stress intensity for crack arrest, K_{I_a}, rather than K_{I_c}, the critical stress intensity for catastrophic failure, while the latter involves indentation and breaking by flexure and results in a measurement of K_{I_c}. The indentation strength technique is based on the same general analysis as the crack indentation technique; however, the crack size can be eliminated from the equation so that only indent load, strength, elastic modulus E, and hardness, H, need to be known to determine the toughness of the material. The equation developed by Anstis et al.[16] is:

$$K_c = 0.59\,(E/H)^{1/8}\,(\sigma\,P^{1/3})^{3/4} \qquad (1)$$

This equation involves a correlation factor (0.59) which is obtained experimentally from traditional ceramics and may not be valid for MDF cements. Fractography is another technique for evaluating fracture toughness. Once we locate and measure the flaws on the fracture surface, we can determine fracture toughness by using the principles of fracture surface analysis:[17,18]

$$K_c = 1.65\,\sigma\,(c)^{1/2} \qquad (2)$$

where $c = (a\,b)^{1/2}$ and a is the crack depth and 2b is the crack width. The constant accounts for the shape and location of the crack on the surface with local residual stress due to indentation.

TABLE 1. Composition of MDF cements.

	A	B
Cement	OPC	Pyrament*
Cement (wt.%)	83	78.5
Water	14	13
Glycerin	0	0.5
Polyacrylamide	3	8
Particle Size (μm)	20	6

*Note that the Pyrament cement contains about 50% alkali-activated ordinary portland cement (OPC).

RESULTS AND DISCUSSION

The results of fracture toughness, as a function of indent load for these two batches of MDF cements, are shown in Figure 1. We observe that the resistance to fracture increases with increasing crack size. Thus, it can be interpreted in two ways. Either the equation does not apply to these materials or there is an "R-curve" behavior for OPCs. In order to determine which of these is the case, we examined the fracture surface of these specimens, and as can be seen in the figure, the values calculated using this technique (fractography Eq. (2)) and the strength-indentation technique (Eq. (1)) coincide well for batch-A which contains less polymer than batch-B. Although this is not a true proof of the validity of the two techniques, it certainly indicates that the toughness does change with crack size, since the latter technique measures the crack size and calculates the toughness based on this measurement and strength. To test the applicability of the indentation-strength method to MDF cements, one can also plot strength versus indent load in logarithmic coordination (not shown here). At loads above 75 N, batch-A showed approximately a straight line with slope = -1/3, indicating a valid test,[6] while for batch-B, the straight line was not observed. The reason for this is unclear. The thickness of our specimens is about 3 mm too thin to tolerate indent loads above 150 N; thicker samples are needed for further investigation. The ultimate toughness for batch-A was taken as the value at the plateau region to be 1.3 MPa $m^{1/2}$ and 2.2 MPa $m^{1/2}$ for batch-B.

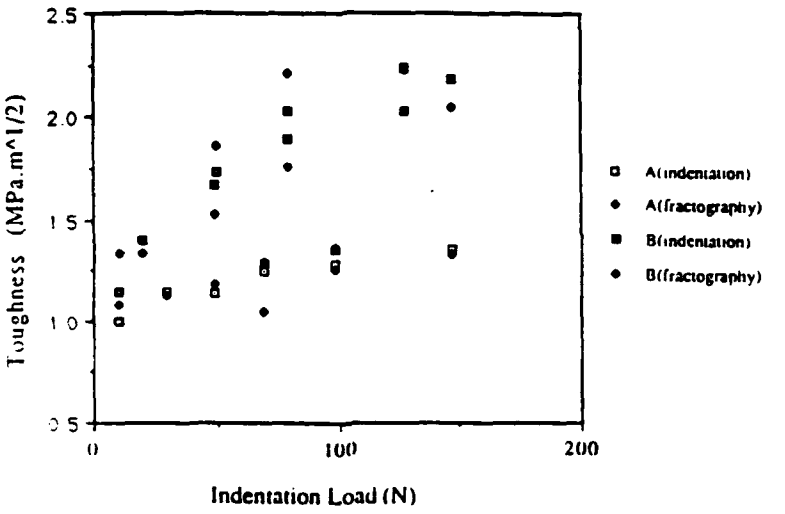

FIGURE 1. Fracture toughness of MDF cements showed an increase with increasing indent loads.

It was also observed that the fracture toughness of batch-B is higher than that of batch-A. The former contained 8 wt.% of polymer, while the latter contained 3 wt.%. It is likely that the toughness increases with the increase of polymer content neglecting that these two batches of MDF cements have a different cement-to-water ratio and composition of cement which certainly affects the mechanical properties.[9] Despite the difference in ratio and composition of cement, we found their microstructures were also different. The low-polymer content cement showed a microcracking fracture surface, while the high-polymer content cement showed a sponge-like microstructure, as seen in Figure 2. The formation of microcracking in many ceramics has been attributed to the thermal expansion mismatch and leads to a toughening effect. We suspect that microcracking is the toughening mechanism for low-polymer content cements. Further investigation is needed to clarify the onset of microcracking prior to loading. While in high-polymer content cement, the fracture surface showed less microcracking in the sponge-like microstructure. The pores are homogeneous and very fine (about 1 μm). We expected that those sponge-like structures contain a large amount of polymer. Upon loading, they work like a crack-arrester and are easily deformed. This leads to a higher toughening effect than that of microcracking.

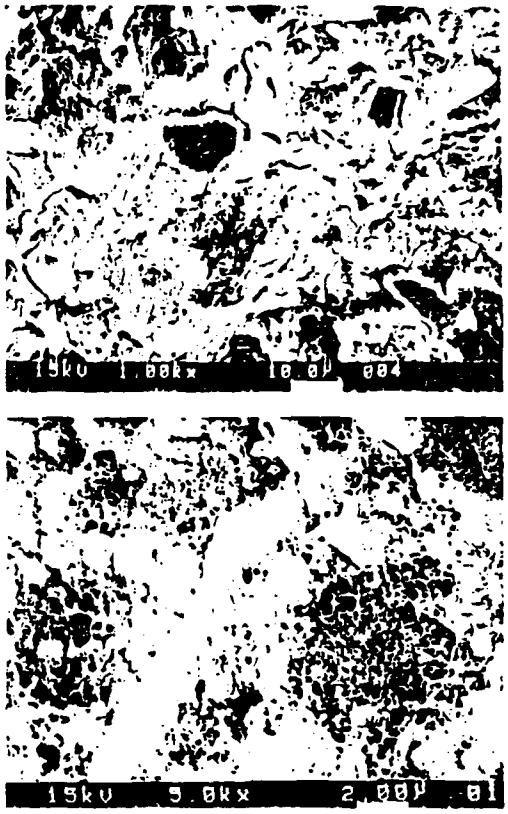

FIGURE 2. Microstructure of MDF cements showed extensive microcracking for batch-A (3 wt.% polymer, upper) and sponge-like structure for batch-B (8 wt.% polymer, below).

CONCLUSION

The indentation-strength technique and fracture surface analysis were found applicable to MDF cements for measuring fracture toughness. Therefore, we suggest that small crack techniques are applicable for the measurement of crack growth resistance in cementitious materials, as long as the crack size is larger than a characteristic dimension of the microstructure. Different microstructures have been observed. Their effects on toughening have been discussed.

ACKNOWLEDGMENT

This work was supported at the Air Force Office of Scientific Research under Contract No. AFOSR-88-0184; technical monitor Dr. Liselotte J. Schioler.

REFERENCES

1. Y. S. Jeng and S. P. Shah, in Very High Strength Cement-Based Materials, edited by J. F. Young (Mater. Res. Soc. Proc., 42 (1985)), pp. 89-100.
2. D. M. Roy and G. M. Idorn, MRS Symposium, op. cit., pp. 133-142.
3. R. Baggott and A. Sarandily, ibid., pp. 69-77.
4. D. M. Roy, Science, 235, 651-658 (1987).
5. G. R. Anstis, P. Chantikul, B. R. Lawn, and D. B. Marshall, J. Am. Ceram. Soc., 64(9), 533-538 (1981).
6. P. Chantikul, G. R. Anstis, B. R. Lawn, and D. B. Marshall, ibid., 539-543.
7. R. F. Cook, B. R. Lawn, and D. B. Marshall, J. Am. Ceram. Soc., 68 (1985).
8. J. J. Mecholsky, in Fractography of Glasses, edited by R. C. Bradt and R. E. Tressler, Plenum Press, in press.
9. N. B. Eden and J. E. Bailey, J. Materials Science, 19, 150-158 (1984).

APPENDIX III

T. Nagira, S.A. Warner, J.J. Mecholsky, and J.H. Adair, "Chemical Processing of Metal Alkoxide Derived Calcium Silicate Chemically Bonded Ceramics," Ibid., Volume 13. Advanced Cements and Chemically Bonded Ceramics, M. Daimon, S. Somiya, G. Sudoh. and K. Takemoto (senior editors), pp.255-262, 1989.

Proceedings of the MRS International Meeting on Advanced Materials

Volume 13

Advanced Cements and Chemically Bonded Ceramics

May 31-June 1, 1988
Sunshine City, Ikebukuro,
Tokyo, Japan

Executive Editors

Masao Doyama, Nagoya University, Nagoya, Japan
Shigeyuki Somiya, The Nishi Tokyo University, Tokyo, Japan
Robert P.H. Chang, Northwestern University, Evanston, Illinois, U.S.A.

Senior Editors

Masaki Daimon, Tokyo Institute of Technology, Tokyo, Japan
Shigeyuki Somiya, The Nishi Tokyo University, Tokyo, Japan
Giichi Sudoh, Chichibu Cement Co., Ltd., Tokyo, Japan
Kunihiro Takemoto, Onoda Cement Co., Ltd., Tokyo, Japan

MRS MATERIALS RESEARCH SOCIETY
Pittsburgh, Pennsylvania

CODEN: MRSPDH

Published by

Materials Research Society
9800 McKnight Road
Pittsburgh, Pennsylvania 15237
Telephone (412) 367-3003
Facsimile (412) 367-4373

ALKOXIDE DERIVED CALCIUM SILICATE CHEMICALLY BONDED CERAMICS

T.NAGIRA, S.A.WARNER, J.J.MECHOLSKY AND J.H.ADAIR
Materials Research Laboratory, The Pennsylvania State University
University Park, PA 16802, U.S.A.

ABSTRACT

Metalorganic decomposition(MOD)is used to obtain fine powers at low temperature for advanced and electronic ceramics. In the present research, powders in $CaO-SiO_2$ system are synthesized by MOD. Physical properties and hydration reactivity of the powders are discussed in terms of C/S ratio ad calcination temperature. Dense chemically bonded ceramics are formed with the powders.

INTRODUCTION

In the past decade, significant advances in flexure strength of cements have been made by eliminating large pores in the structure [1-4]. The high strength cements, known as macro defect-free cements(MDF cements), are produced by high shear mixing of cement powder with polymer additions at low water to solid ratios to increase flexure strength from 5MPa for conventional cements to 150MPa. This value is comparable to those of sintered ceramics. Therefore, MDF cements are a kind of ceramics formed by hydration (chemical bond). Generally, dense and high strength ceramics formed by chemical bonds are defined as chemically bonded ceramics (CBC).

But MDF cements for which conventionally produced cement powders were used still included residual pores in diameter up to 15um in hydrated bodies. Birchall et. al. explained the strength of cement-based materials by Griffith theory in which the tensile or bending strength of brittle materials is inversely proportional to critical flaw size[1]. According to fracture mechanics theory, it is possible to achieve larger strength than that of MDF cements by eliminating several to 15um pores using fine cement particles such as submicron size for better compaction in green bodies.

Fine powder syntheses by chemical processes which lead to lower temperature crystallization and denser structure of ceramics than conventional methods have been increasingly applied to electronic and advanced ceramics[5]. However, there are few reports which described novel low-temperature syntheses of cement compounds [6]. The process could reduce high calcination temperature in conventional cement manufacturing process and produce fine cement powders.

Therefore, this research focused on
1)Preparation of hydraulic calcium silicate by chemical process such as metalorganic decomposition (MOD).
2)Producing cements with dense structure and high strength.

MRS Int'l. Mtg. on Adv Mats. Vol. 13 © 1989 Materials Research Society.

MATERIALS AND METHODS

Powder Preparation

Calcium silicate powders are synthesized by MOD method. Ca-ethoxide was prepared by refluxing ethanol with Ca metal. Tetramethyloxysilane(TMOS) was used to provide the source of silicon.

TMOS was diluted in ethanol and refluxed for an hour. Ca metal was added to the solution followed by 4 hours refluxing. Since small amounts of Ca metal remained unreacted after refluxing, they were removed by centrifugation to obtain homogeneous solutions. Half of the stoichiometric amount of deionized (D.I.) water for hydrolysis of Ca ethoxide and TMOS was mixed with the alkoxide solution followed by vigorous stirring for 18 hours. Then, thirty times the stoichiometric amount of ammonianized D.I. water (pH 10) was added to the partially hydrolyzed alkoxide solution with refluxing for 24 hours to obtain precipitations. All of the processes described above were performed under a nitrogen atmosphere.

Precipitations were washed with ethanol and dried at 80°C under vacuum. Dried powers were heat treated at 550°C, 700°C and 800°C for an hour.

Powder Characterization

CaO/SiO_2 (C/S) mole ratio was analyzed by x-ray fluorescence (XRF). Thermal gravimetric analysis (TGA) was performed up to 1050°C to measure weight loss. Surface area and particle size distribution were measured by BET method and a light scattering method, respectively. Microstructures of powders were observed by scanning electron microscope (SEM). X-ray diffractometry was used to characterize crystalline phases. The heat of hydration of the powders was measured by calorimetry.

Preparation of pellets

Calcined powders with C/S ratio equal to 2.0 were uniaxially pressed at 345MPa into disks 1.8cm in diameter. 0.3g of powder was used for each pellet.

Pellets were placed in $Ca(OH)_2$ saturated water at 60°C and cured up to 15 days. After specific curing times, pellets were dried at R.T. under vacuum for 5 hours and analyzed by XRD and SEM to follow hydration process.

RESULTS AND DISCUSSION

Powder Characterization

Fig. 1 summarizes the results of the XRD analysis for powders prepared by MOD(MOD powder) calcined at various temperatures. Calcium silicate crystalline phases obtained at C/S ratio more than 2.0 were β-C_2S and α'-C_2S. They were crystallized at 600°C and α'-C_2S disappeared at 800°C. Excess calcium over C/S ratio of 2.0 was separated as hydroxide, carbonate or oxide depending on calcination temperature. On the other hand, only β-C_2S was crystallized around 600°C at C/S ratio equal or less than 2.0. No other calcium compound was detected for these conditions.

Fig.2 shows XRD patterns of MOD powders with C/S ratio of 2.0(a) and 2.8(b) calcined at various temperatures. At C/S ratio of 2.0(a), a small peak of β-C_2S appeared around 32.2° at 600°C and β-C_2S was crystallized well at 700°C. No crystalline phase was detected except for β-C_2S. At C/S ratio of 2.8(b), a peak of α'-C_2S was also seen around 33.4° which disappeared at 800°C while β-C_2S increased crystallinity with the increase of calcination temperature. At the later C/S ratio, $Ca(OH)_2$ was crystallized at 80°C, was converted to $CaCO_3$ at 550 and to CaO at 700°C.

Fig.3 shows the TGA results for as-dried (80°C) MOD powders. The heating rate was 10°C/min. Four different weight loss regions were found in the curves. The first one is from R.T. to 200°C which is derived from vaporization of water and organic. The second one occurred around 400°C. Decomposition of organic probably contributes to this loss. The third one between 550 and 700°C is the largest. Considering the decomposition temperature of $Ca(OH)_2$ (i.e., 580°C), it is probable that third loss is caused by evolution of structural water. The last loss which begins at 750°C probably derives from the decomposition of $CaCO_3$. Small third and fourth losses for the lowest C/S ratio of 1.7 compared to those for other ratios can be related to the fact that neither $Ca(OH)_2$ or $CaCO_3$ was detected by XRD. The $CaCO_3$ contents based on the results in Fig.3 were less than 1 weight % for C/S ratio of 1.7 and about 3 weight % for C/S ratio of 2.2, 2.8 and 3.1.

The MOD powders showed the surface areas of 50 to 100m^2/g even after the 700°C calcination. On the other hand, mean particle sizes of MOD powders were in the range of 5 to 20um. The values measured by light scattering are much larger than those expected from surface areas measured by BET. Therefore, the particles detected by light scattering are agglomerates composed of submicron particles. However, specific relationship was not found between C/S ratio and surface area or particle size.

SEM pictures in Fig.4 show the nature of the agglomerate. The powder shown here was calcined at 600°C with C/S ratio of 2.0. At low magnification (a), a wide distribution of particle size was observed up to 10um. At high magnification(b), agglomeration of particles in diameter below 0.1um was seen. This porous structure causes high surface area.

Hydration of MOD powders

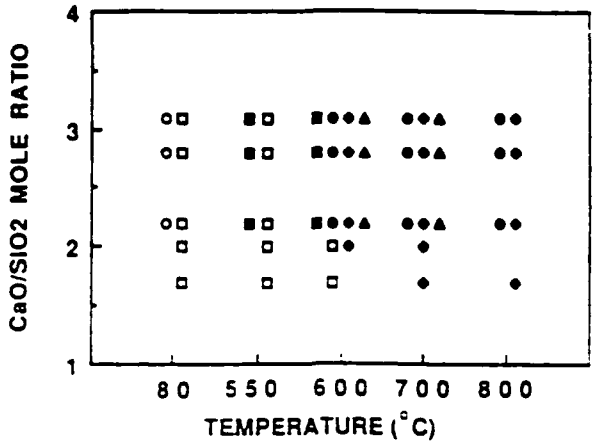

Fig. 1. XRD results of MOD powders calcined at various temperatures.
□ ; amorphous, ■ ; $CaCO_3$, ○ ; $Ca(OH)_2$, ● ; CaO, ◆ ; β-C_2S, ▲ ; α'-C_2S.

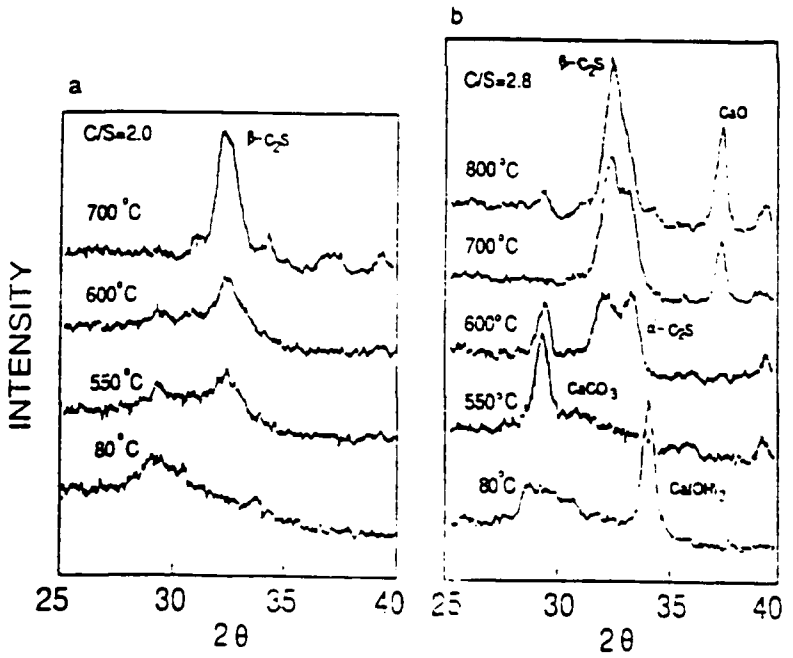

Fig. 2. XRD patterns of MOD powders with C/S ratio of 2.0 calcined at various temperatures.

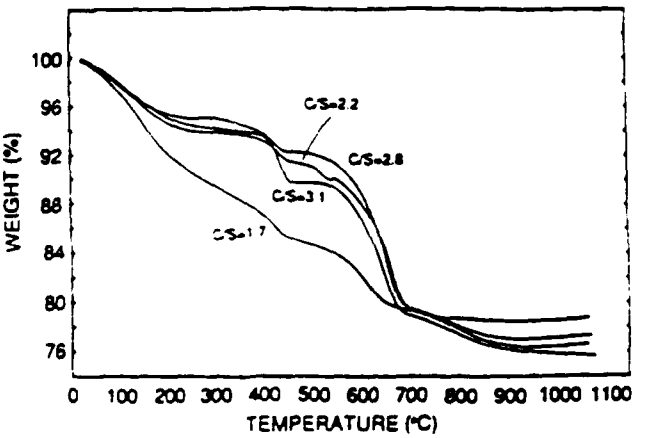

Fig. 3. TGA results of as-dried (80°C) MOD powders with various C/S ratios.

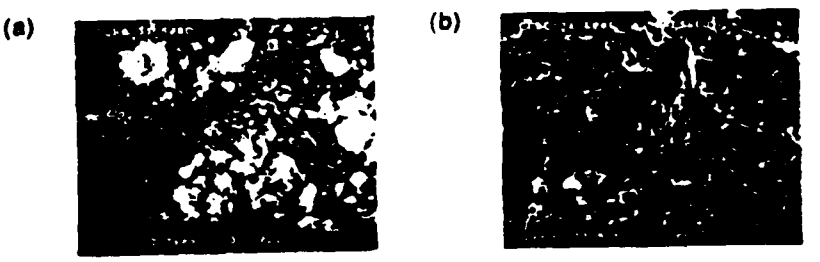

Fig. 4. Scanning electron micrographs of MOD powder calcined at 600°C with C/S ratio of 2.0.
(a); in low magnification, (b). in high magnification.

The calorimetry results for MOD powders are listed in Table 1. Two peaks were observed in the diagrams of rate of heat evolution versus hydration time similar to C_3S[7,8]. The first one appeared a minute after the beginning of hydration and the second 5 to 44 hours later depending on C/S ratio and calcination temperature. The higher the C/S ratio and calcination temperature, the earlier the second peak appeared. As powder with higher C/S ratio contains more CaO, higher CaO content seems to affect earlier hydration. The effect of calcination temperature on delaying second peak is quite large at 700°C. Based on the XRD results summarized in Fig. 1, the development of crystalline phase (β-C_2S) probably contributes to delay of the second peak.

The heat rate of the first peak increased with increasing C/S ratio. The heat rate of the second peak is more dependent on calcination temperature than C/S ratios. Significant decrease of the heat rate at 700°C can be related to both the presence of β-C_2S and decreased surface area. The values at 550 or 600°C (5-6 cal/g·h) are in the same range as those of C_3S (3-6 cal/g·h), but even larger than those of β-C_2S (0.5-1 cal/g·h) [9,10].

Fig. 5 shows the hydration of pellets formed with MOD powders calcined at 700°C. At C/S ratio above 2.0, both CSH and $Ca(OH)_2$ were detected as hydrates while, below or equal to 2.0, only CSH was present. Increase in the XRD peaks for $Ca(OH)_2$ was also observed with increased C/S ratio. β-C_2S still existed at lower C/S ratios after two days of hydration. The results for MOD powders calcined at 550 and 600°C, which are not shown here, indicate the same pattern as in Fig. 4 except that β-C_2S did not exist even after two days hydration. Thus, it is established by these results that MOD powders have high reactivity with water and those containing CaO or amorphous phase complete hydration earlier.

Fig. 6 shows SEM pictures of the fractured surface of a pellet which was formed with MOD powder calcined at 600°C with C/S ratio of 2.0 and cured for two days. It shows dense structures with infrequent pores in the micron size at low magnification (a). At high magnification (b), a pore of lum size is seen but it is surrounded by well densified structures which are much different from the porous structures of the unhydrated powder in Fig. 4 (b).

CONCLUSION

Powders in CaO-SiO_2 system with very high surface areas greater than $50m^2/g$ even after 700°C calcination were synthesized by MOD. α'-C_2S and β-C_2S were crystallized when C/S is greater than 2.0, but only β-C_2S when C/S ratio is equal to or less than 2.0 as for calcium silicate phase. No crystalline calcium silicate was observed below 550°C. MOD powders, especially those containing an amorphous phase, showed high reactivity with water. Dense CBC's were formed by uniaxially pressing MOD powders and hydrating them at 60°C.

Table 1. Heat evolution of MOD powders mixed with water at water to solid weight ratio of 1.

Sample	Time of 1st Peak (min.)	Heat Rate of 1st Peak (cal/g·h)	Time of 2nd Peak (h)	Heat Rate of 2nd Peak (cal/g·h)
C/S=2.0				
550 °C	1	130	14	6.0
600 °C	1	170	17	5.7
700 °C	1	200	44	1.1
C/S=2.4				
550 °C	1	600	10	4.3
600 °C	1	350	8	5.6
700 °C	1	260	20	1.5
C/S=3.1				
550 °C	1	1000	5	5.1
600 °C	1	970	7	3.3
700 °C	1	1200	11	0.9

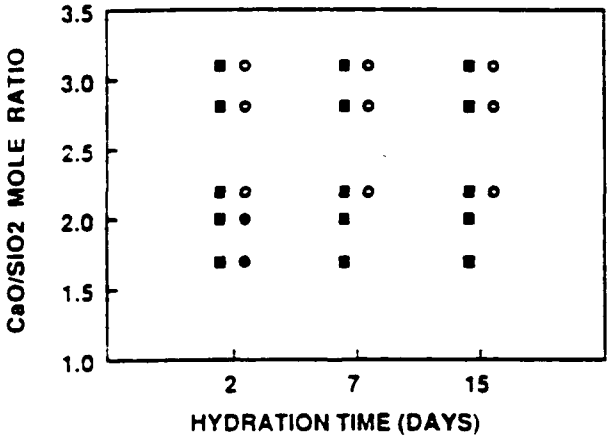

Fig. 5. Hydration of pellets formed with MOD powders calcined at 600°C.
■ CSH ○ Ca(OH)2 ● β-C2S

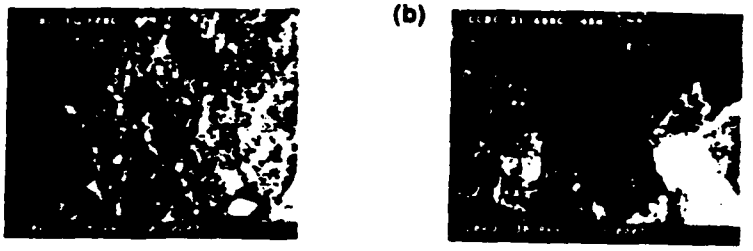

Fig. 6. Scanning electron micrographs of fractured surfaces of a pellet formed with MOD powder and hydrated for 48 hours. The calcination temperature and C/S ratio of the powder are 600°C and 2.0, respectively. (a); in low magnification, (b); in high magnification.

REFERENCE

1. J.D.Birchall, A.J.Howard and K. Kendall, Proc. Brit. Ceram. Soc., 32, 25-32 (1982)
2. K.Kendall, A.J.Howard and J.T.Birchall, Phil. Trans. R. Soc. Lond., A310, 139-153 (1983)
3. J.D.Birchall, A.J.Howard and K.Kendall, Nature, 289, 388-390 29 January (1981)
4. N.McN.Alford, Cem. Concr. Res., 11, 605-610 (1981)
5. K.S.Mazdiyasni, Ceram. Inter. 6, 45-56 (1982)
6. D.M.Roy and S.O.Oyfesobi, J. Amer. Ceram. Soc., 60, 178-180 (1977)
7. R.Kondo and M.Daimon, ibid, 52, 503-508 (1969)
8. H.M.Jennings, B.J.Dalgleish and P.L.Pratt, ibid, 64, 567-573 (1981)
9. I.Older and J.Schuppstuhl, Cem. Concr. Res., 11, 765-774 (1981)
10. S.Shibata, K.kishi and M.Daimon, ibid, 14, 323-328 (1984)

APPENDIX IV

P.M. Heiland, Processing and Properties of Chemically Derived Calcium Silicate Cement, Master of Science, Solid State Science, May, 1990.

The Pennsylvania State University

The Graduate School

PROCESSING AND PROPERTIES OF CHEMICALLY DERIVED CALCIUM SILICATE CEMENT

A Thesis in

Solid State Science

by

Petra Maya Heiland

Submitted in Partial Fulfillment
of the Requirements
for the Degree of

Master of Science

May 1990

Abstract

This thesis demonstrates processing and properties of chemically derived calcium silicate cements. Chemical synthesis and processing methods offer the opportunity to improve the strength of cement. Chemically derived calcium silicate was synthesized from metal organic decomposition and hydrothermal methods. The chemically derived fine particles are then used to produce cements by uniaxial pressing, extrusion or isostatic pressing. These cements can potentially have critical flaws less than 10 microns as opposed to critical flaw sizes greater than 100 microns in conventional cement.

An iterative approach was established to determine the relationship among processing conditions, microstructure, and mechanical properties to produce higher strength cement. Most studies on cements have focused on either processing or mechanical properties. In this thesis the cements were synthesized and processed using chemical techniques. Mechanical properties and origin of critical flaws were determined, and subsequent processing iterations were designed to eliminate flaws. Much progress was made towards this goal, but optimum bend strengths were not achieved. Further iterations must be made in order to increase the strength of the cement.

Table of Contents

Table of Contents (Continued)

APPENDIX V

S. Venigalla, P.M. Heiland, B.E. Scheetz, and J.H. Adair, "Crystal Growth Modeling of Hydrothermally Derived Calcium Silicate Hydrates," to be submitted to J. Am. Ceram. Soc.

ROUGH DRAFT

CRYSTAL GROWTH MODELLING OF HYDROTHERMALLY DERIVED CALCIUM SILICATES

S.Venigalla[1], P.M. Heiland[2], B.E. Scheetz[2], and J.H. Adair[1]
[1] Department of Materials Science and Engineering, University of Florida, Gainesville, FL 32611.
[2] Materials Research Laboratory, The Pennsylvania State University, University Park, PA 16802.

HYDROTHERMAL PRECIPITATION OF CALCIUM SILICATES

Hydrothermal reactions are generally carried out in stainless steel or teflon lined pressure vessels at elevated temperatures. The quantity of water used in these vessels is always such that both liquid and vapor phases are present for synthesis of calcium silicates above 100°C up to the critical point of water, 374°C. The solubilities of both lime and silica are small such that the pressure developed is practically equal to the saturated vapor pressure of steam at the operating temperature. CaO is prepared by heating analytical grade $CaCO_3$[1] at 1000°C for 16 hours. High purity quartz[2] (99.14% SiO_2, 5 μm average particle size) is used as the silica source. The quartz and CaO are added such that a ca/si ratio of 0.83 is achieved. Figure shows the flow chart for the hydrothermal synthesis. All reactions were carried out at saturated steam pressure in a 23 ml safety sealed steel vessel[3] with a teflon lining. After hydrothermal treatment, the reaction mixtures are filtered and the solid which remains is generally washed with water and dried in a vacuum dessicator.

Phase identification of the synthesized powders is performed on an automated X-ray powder diffractometer[4]. All scans are run from 4 to 56 degrees 2θ at a rate of 2 degrees per minute. Scanning electron microscopy[5] is used to determine the microstructure and morphology of the powders.

---

[1] Fisher Scientific, Fair Lawn, NJ.
[2] Minsul Quartz, Berkley Spring, WV
[3] Parr Bomb 276AC, Parr Instrument Company, Moline, IL.
[4] Scintag PAD V, Santa Clara, IL.
[5] International Scientific Instruments (ISI) DS-130, Milptas, CA.

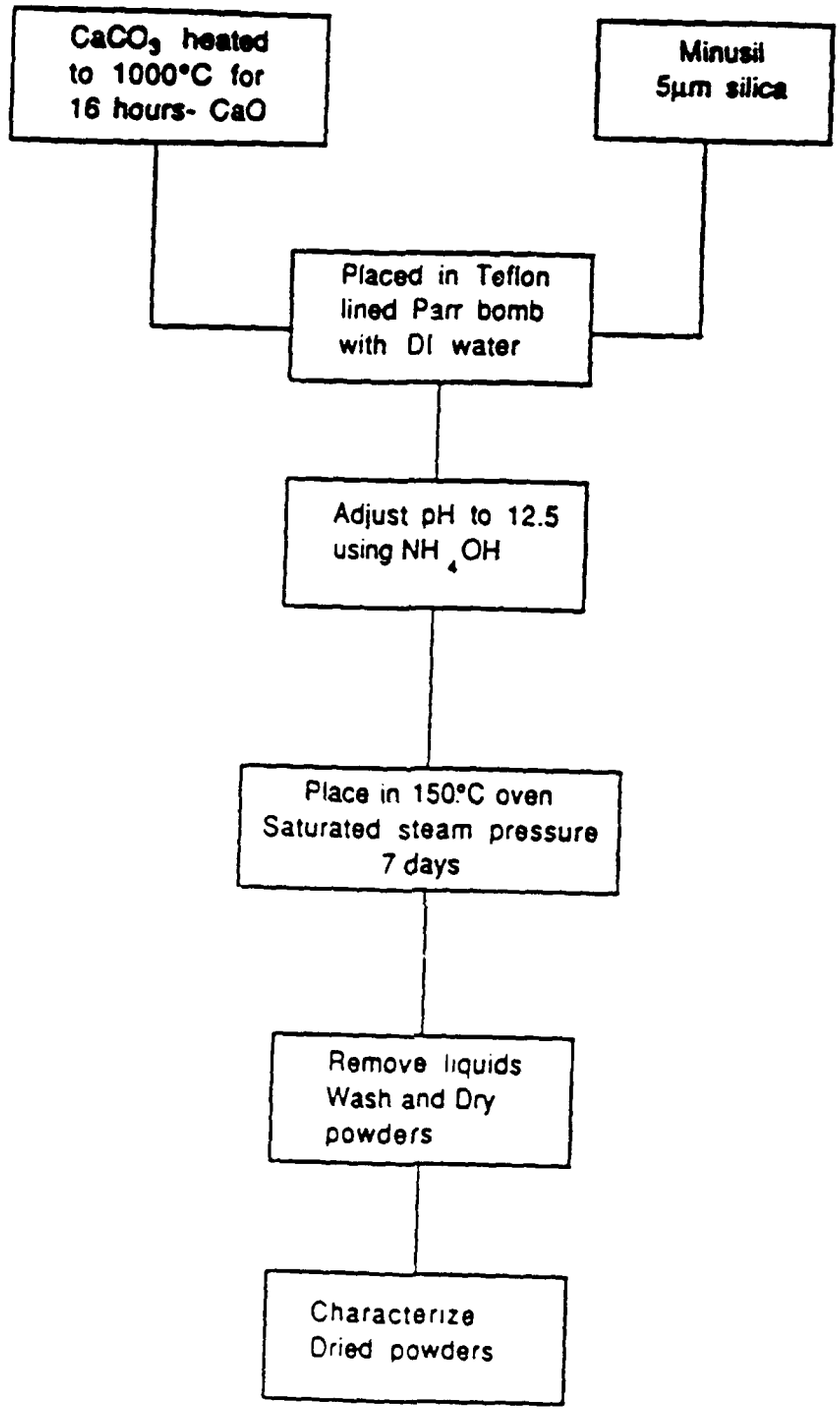

Figure . Schematic chart illustrating the processing steps involved in the hydrothermal synthesis of calcium silicate powders.

STRUCTURE AND MORPHOLOGY

There are many calcium silicate phases which may result from hydrothermal treatment of lime and silica[]. The two phases closest to tobermorite in the same Ca:Si and temperature ranges are gyrolite and xonotlite.

Gyrolite $(Ca_4)(Si_6O_{15})(OH)_2 \bullet 3H_2O$ can be distinguished from tobermorite and xonotlite from the 22 Å d-spacing. The gyrolite group is comprised of compounds forming hexagonal or pseudohexagonal crystals with a (0001) cleavage similar to mica and an a-axis of 9.7 Å. Gyrolite is easily synthesized within temperatures of 120-240°C [].

Xonotlite $(Ca_6)(Si_6O_{17})(OH)_2$ also occurs as a natural mineral. Xonotlite has a lime-silica-water ratio of 3:3:1. Xonotlite is formed reproducibly when any sufficiently reactive starting material of 1:1 Ca/Si is treated hydrothermally at 150-400°C under saturated steam pressure conditions. Its formation from lime-silica mixtures proceeds through intermediate stages of C-S-H and tobermorite. Xonotlite forms prismatic crystals or fibrous aggregates with elongation parallel to the b-axis. The crystal structure was determined by Mamedov and Belov [] who found that double drierketten (metasilicate chains) of empirical formula $(Si_6O_{17})^{12-}$ were present together with Ca^{2+} and OH^- ions.

Tobermorite as a family of phases has characteristic basal spacing of 9.3, 11.3 and 14.0 Å as determined by x-ray diffraction. These basal reflections represent the thickness of the elementary layers. The 11 Å variety has a Ca/Si ratio of 0.83 and can be easily synthesized below 140°C. The 11 Å variety of tobermorite can be described as normal if the basal spacing decreases to 10 Å or less on heating at 300°C or anomalous if the spacing does not decrease below 11 Å under the same conditions. According to Megaw and Kelsey[] the crystal structure of 11 Å tobermorite contains two identical complex layers which are parallel to the (001) direction and which fit together with a center of symmetry. Each layer has two central sheets of composition 4CaO. These are arranged so that each calcium has four oxygen neighbors in its own sheet and two in the sheet at the next level. Each pair of adjacent oxygens forms an edge of a tetrahedron containing silica. These tetrahedras are joined into chains that are parallel to the b-axis. This structure can either be plate-like or fibrous. Figure shows the scanning electron micrographs of the hydrothermally derived tobermorite and xonotlite particles. Notice the mixed fibrous and plate-like morphology of tobermorite.

A

B

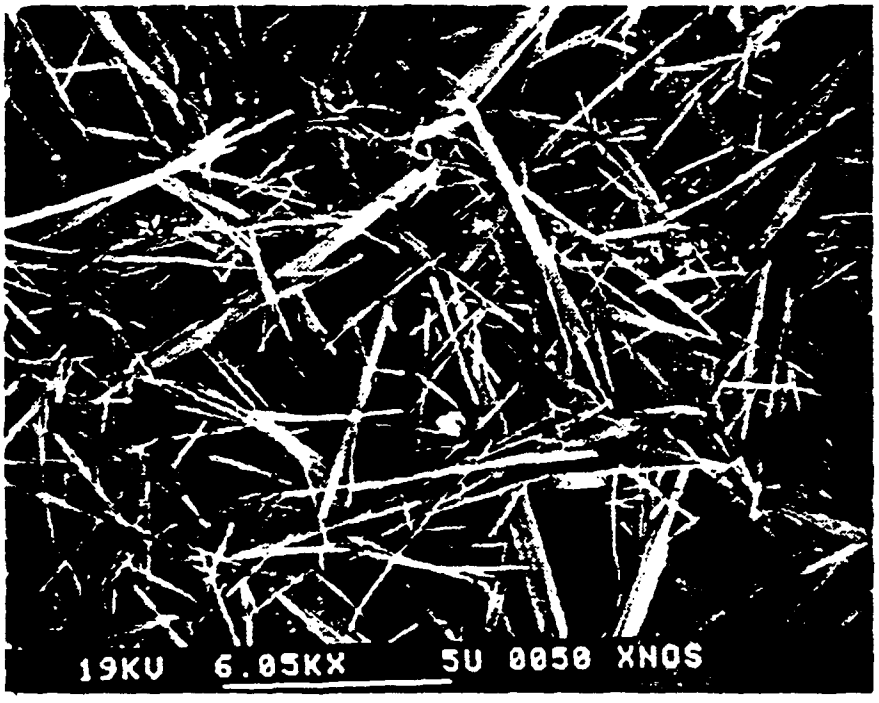

Figure . Scanning electron micrographs of hydrothermally derived calcium silicates: A) Tobermorite, exhibiting mixed plate-like and fibrous morphology, and B) Xonotlite, with fully fibrous morphology.

MODELLING OF GROWTH HABITS

The computer simulation of crystal growth habits has been carried out using the SHAPE® program. To draw an individual crystal using this program, it is necessary to enter the crystal class, the point group, the corresponding unit cell parameters, and the indices and central distance for one face of each form. From the crystal class and point group, the program determines what symmetry operators to use in the calculations, and generates all the faces belonging to each form. The central distance is the perpendicular distance from the center of the crystal to the faces of the corresponding form. The greater the distance, the less prominent the form (the smaller the area of the faces of that form in the final shape). The following crystallographic data has been used to generate the single crystal shapes of calcium silicates[].

Crystal Lattice: Orthorhombic

Lattice Parameters (nm): a = 0.564, b = 0.368, c = 2.26

Point Group: 222

The crystallographic forms specified for the individual shapes are listed in Table 1.

Table 1. Crystal forms and corresponding central distances used to generate individual single crystal shapes of calcium silicates.

FORMS	INDICES	For plate-like structure: CENTRAL DISTANCE	For fibrous structure: CENTRAL DISTANCE
1	1 -1 1	1.00	1.00
2	1 1 1	1.00	1.00
3	1 1 0	0.10	1.00
4	0 2 1	1.00	1.00
5	1 -2 0	1.00	1.00
6	1 0 1	1.00	1.00
7	0 1 0	1.00	0.10

The resulting shapes for both schemes are illustrated in Figure . Crystal growth habit on the (110) prism planes leads to a fibrous structure of the particles with very large aspect ratios, whereas the growth habit on the (010) basal planes results in a plate-like structure of the particles.

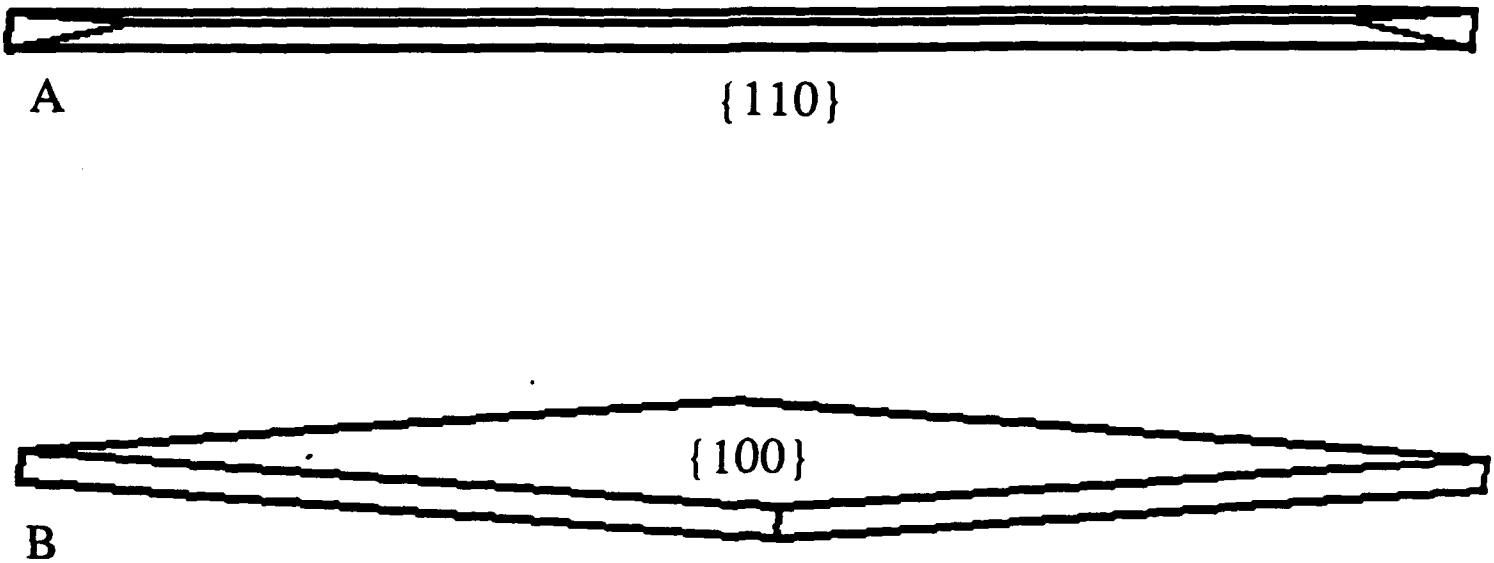

Figure . Simulated single crystal shapes of calcium silicates generated by SHAPE®.
A) Crystal growth habit on {110} prism planes leading to a fibrous morphology, and
B) Crystal growth habit on {100} basal planes leading to a plate-like morphology.

APPENDIX VI

Kelly Markowski, A Fundamental Study of the Surface Chemistry of Calcium Silicate Hydrate, Bachelor of Science Thesis, Ceramic Science and Engineering, The Pennsylvania State University, May, 1990.

The Pennsylvania State University
College of Earth and Mineral Sciences
Department of Materials Science & Engineering

A Fundamental Study of the Surface Chemistry of Calcium Silicate Hydrate

A Thesis in
Ceramic Science & Engineering
by
Kelley Markowski

Submitted in Partial Fulfillment of the
Requirements for the degree of

Bachelor of Science
May 1990

Approved:

7 May 1990

Signatures:

Dr. James Adair
Assistant Professor
of Ceramic Science
and Engineering

7 May 1990

Dr. Kari Spear
Program Chairman

Abstract

This thesis investigates the properties of tobermorite, a form of calcium silicate hydrate that comprises the binding fibers in normal Portland cements. The properties studied were: the zeta potential and isoelectric point of tobermorite in various concentrations of $CaCl_2$, the mobility of tobermorite in these solutions; and the amount of calcium and carbonate liberated for pH values between 7 and 13.

The zeta potential was found to become more negative for samples in $CaCl_2$ solutions than in samples prepared in deionized decarbonated water. The zeta potential behavior is listed below (all measurements were taken for pH values between 7 and 13):

a) deionized, decarbonated water — average zeta potential = -0.325
b) 10^{-2}M $CaCl_2$ — average zeta potential = -3.90
c) 10^{-3}M $CaCl_2$ — average zeta potential = -6.65
d) 10^{-4}M $CaCl_2$ — average zeta potential = -10.75

This behavior is attributed to the specific adsorption of Ca^{2+} ions in solution.

The isoelectric points increased when $CaCl_2$ was added to solutions. due to shifts in zeta potential, the isoelectric point for 10^{-4}M $CaCl_2$ was higher than anticipated, this unanticipated result

is attributed to carbonate contamination. The isoelectric points obtained are listed below:

a) deionized, decarbonated water	isoelectric point = 10.33
b) 10^{-2}M $CaCl_2$	isoelectric point = 10.95
c) 10^{-3}M $CaCl_2$	isoelectric point = 10.47
d) 10^{-4}M $CaCl_2$	isoelectric point = 11.63

The mobility was also investigated and was found to reach a minimum value at the isoelectric point due to increased coagulation.

Finally, the calcium and carbonate concentrations were investigated as a function of pH. The calcium concentration was found to be a maximum at low pH values indicating the dissociation of tobermorite. The calcium concentration was also found to vary inversely with carbonate concentration, due to the formation of calcium carbonate.

Table of Contents

APPENDIX VII

P.M. Heiland, J.H. Adair, B.E. Scheetz, Y.-S. Chou, and J.J. Mecholsky, "The Use of Gel-casting in the Fabrication of High Strength Chemically Bonded Ceramics," to be submitted to J. Cement Concrete Res.

ROUGH DRAFT

The Use of Gelcasting in the Fabrication of High Strength Chemically Bonded Ceramics

P.M. Heiland, J.H. Adair. B.E. Scheetz, Y.-S. Chou, and J.J. Mecholsky

Pennsylvania State University
University Park, Pennsylvania

Abstract

An unconventional method for processing calcium silicate cement is described. Gel casting has been applied to other materials, such as alumina, but not to cements (1). Gel casting uses a monomer solution which can be polymerized to form a strong, polymer-solvent gel. The monomer solution provides a low viscosity vehicle for carrying the ceramic powder and the crosslinked polymer gel provides a mechanism for permanently immobilizing the ceramic slurry in the desired shape. Because the gelled vehicle contains only 10-20 wt% polymer the solvent can be removed readily from the gelled part by a relatively simple drying step. Also, because the polymer in the gel is crosslinked it cannot migrate with thee solvent during drying. Gel casting is a complicated technique involving several steps. The first step is to determine which monomer and initiator will be used for polymerization. The second step is to mix the cement with the monomer and uniaxially press the samples to give them shape. The samples were then isostatically pressed to densify the sample. The cured samples were tested for mechanical properties and the relationship between processing and properties was determined.

Introduction

Gel casting is a term referring to any process for forming ceramic bodies based on the *in-situ* polymerization of monofunctional and difunctional monomers in an aqueous solution. One advantage of gel casting in the case of hydraulic cement is that less water can be used (<.20 wt%) when mixing the cement slurry. Another advantage is that slurries can

be formed using standard ceramic processing techniques. The difference between gel casting and polymer impregnated concrete is that in the former case the monomer is mixed with the cement before forming, not impregnated into the cement after it has been formed. Forming techniques of gel cast materials include uniaxial or isostatic pressing, casting, extrusion and injection molding (1).

Gel formation by *in-situ* polymerization has been applied to enhanced oil recovery (1). In this method acrylamide monomer (H_2C+$CHCONH_2$), crosslinking monomer (bisacrylamide), ammonium persulfate $(NH)_4S_2O_8$) initiator and a potassium ferricyanide ($K_3Fe(CN)_6$) inhibitor are premixed above the surface and pumped down the oil well. Pumping is easier due to the low viscosity of the monomer solution. This allows for more control of the flow of fluids through the reservoir.

Materials and Methods

OPC as-received and hydrothermally prepared dehydrated calcium silicate (tobermorite) were the two types of cement used for gel casting. The monomer used was acrylamide (97%) from Aldrich. Two polymerization initiators were evaluated, ammonium persulfate $(NH_4)_2S_2O_8$ and potassium persulfate $K_2S_2O_8$, both from Polyscience. A typical batch included 80 wt% cement, 13.95 wt% DI water, 6 wt% monomer, 0.05 wt% initiator. Before the DI water could be used it was flushed with Argon for 12 hours in order to remove any dissolved oxygen. The oxygen acts as an inhibitor to the polymerization of acrylamide.

A premix solution of 70 wt% Ar-DI water and 30 wt% acrylamide monomer was made first. This solution was stored under Ar and used over a period of 2 months. The water to cement ratio needed for gel casting was 0.17 because there is no crosslinking which can inhibit the cement particles from moving passed each other. To 40 grams of cement, 10 grams of premix was added and 0.015 grams of initiator. This slurry was either mixed by hand or with the shear mixer. The slurry was allowed to sit in Ar for 12

hours before pressing. To press, approximately 4 grams of slurry was used. The bars were pressed at 120 MPa and cured at 60°C for 7 days with water, without water, or with $Ca(OH)_2$.

In preliminary experiments, the results of the uniaxial pressing of the cement were unsatisfactory because the microstructure of the samples were inhomogeneous due to incomplete mixing of the mixture and the strength were low (50 MPa). Therefore, the next step taken to reduce critical flaw size was isostatic pressing. In isostatic compression the specimen must be enclosed in a thin, impermeable membrane and compressed by a fluid. True isostatic compression causes a decrease in volume but no shear or distortion.

The set up for isostatic pressing is quite simple. The samples and fluid are placed in a steel cylinder with a sealed cap. A gauge is attached to the cap with capillary tubing in order to monitor the pressure inside the vessel. Argone is pumped into the vessel up to a maximum of 30,000 psi (207 MPa).

Before isostatic pressing the samples were uniaxially pressed to 2900 psi (20 MPa) so that the samples would maintain their shape while being prepared for isostatic pressing. Bars pressed with OPC had similar compositions to those used for uniaxial pressing. Bars pressed with the chemically derived calcium silicate had the same cement:polymer:water ratio as the OPC samples but the compositions of the cements were varied (Table 2).

Table 2: Sample composition and densities of isostatic pressed cement bars.

Sample	Composition[1]
A	80% TOB + 20% XON
B	90% TOB + 10% XON
C	95% TOB + 5% XON
D	100% TOB

[1]TOB = tobermorite, XON = xonotlite

Samples A, B, and C are called self similar composites. The name is given to samples made with the same composition but different phase and structure. The two types of morphology (platelike and fibrous) should enhance the strength of the final cement product.

After the samples were uniaxially pressed to 20 MPa they were placed inside two impermeable membranes. A vacuum was pulled (30 mm Hg) in order to remove the air trapped in the membrane. The samples were then placed in the steel vessel and the air pumped in so that a pressure of 29.9 ksi (206 MPa) was achieved. This pressure was held for one minute then released. The samples were removed from the membranes and placed in DI water in the 60°C drying oven for 7 days.

Results and Discussion

There are many variables affecting the polymerization of a monomer during gel casting. One factor is the type of initiator used for polymerization. A batch using identical amounts of cement and premix was made using different types of initiator. An ammonium persulfate solution containing 7 wt% initiator had a pH of 1.9, the same concentration solution containing potassium persulfate had a pH of 4.5. Since the hydration of cement is dependent on pH it was expected that the potassium persulfate would not inhibit the hydration as much as the ammonium persulfate, and therefore, produce a higher strength product. This turned out to be the case as shown in Table 2. However the difference is negligible.

The strengths were determined using a rather new technique developed by Jack Mecholsky and Y.S. Chou (3).

The OPC used for these experiments was not milled. Therefore, the strengths achieved using gel casting could be much higher if the mean particle size was smaller than 11 μm. In either case the strength achieved is higher than that for conventionally processed cements.

Table 2: Strength as a function of initiator for gel cast OPC samples

Initiator	Avg. Strength (MPa)	
$(NH_4)_2S_2O_8$	54	± 2
$K_2S_2O_8$	56	± 2

The mixing method also affected the final strength of the cement. Two identical batches were made using potassium persulfate as initiator, one mixed by hand and one using the shear mixer. As shown in Table 3 the shear mixed cement had a significantly higher bend strength than that mixed by hand. This was also an expected result because shear mixing produces a more homogeneous mixture, thus eliminating large flaws caused by improper mixing.

Table 3: Strength vs. curing procedure for the gel cast bars.

Mixing Method	Avg. Strength (MPa)	
Hand	54	± 4
Shear	70	± 4

The gel cast OPC was cured under three conditions, in $Ca(OH)_2$, water, and acetone. It was expected that the $Ca(OH)_2$ would keep the pH of the curing solution above 12 to aid in hydration and that the acetone would shrink the polymer and densify the sample (2).

Table 4 gives a summary of the mechanical properties of OPC paste cured and processed at different conditions. The samples cured in $Ca(OH)_2$ solution showed the worst mechanical properties. The surfaces of these bars had long (>1000 μm) cracks. The flaw size was determined using $Kc = 1.65\sigma c^{1/2}$, to get an estimate of a lower bound. These bars had different surface morphology than those cured in water. This implies that either the infiltration of the $Ca(OH)_2$ is not complete or that the green structure after uniaxial pressing has no connected pores. The later alternative, however, is unlikely.

The microstructure of the fracture surface of the samples shear mixed and cured in water were all similar. Most of the cracks were less than 50 μm in length (measured by SEM). Strengths for these samples were as high as 59 MPa with a fracture toughness of 1.4 MPa $m^{1/2}$. The microstructure of the bars cured in acetone also showed large cracks. It was expected that the acetone would have a positive effect on the strength because acetone shrinks and densifies the polymer. Apparently the polymer did shrink, leaving very large pores thus decreasing the strength of the samples.

Table 4: Summary of mechanical properties of OPC paste.

Condition	σ_f(MPa)	K_c(MPa $m^{1/2}$)	Flaw size (μm)[1]
$Ca(OH)_2$	13 ± 1	------*	>1000
	21 ± 1	------*	>1000
Water	55 ± 2	1.41 ± 0.2	387
	59 ± 2	1.43 ± 0.2	326
Acetone	19 ± 1	0.87 ± 0.1	770
	26 ± 1	1.25 ± 0.2	849

[1] Flaw sizes were calculated

* toughness values were too low to be measured

Table 5 gives a summary of the mechanical properties of isostatically pressed samples A-D, which contained varying amounts of tobermorite and xonotlite (See Table 2). The samples were first uniaxially pressed in order to form the bars then isostatically pressed. Table 5 shows the results from the density calculations after isostatic pressing and the % density increase after isostatic pressing. These measurements were made to show that the samples were densified during isostatic pressing. Following curing, the samples were tested for strength by Chou (3). Samples A-D were all broken by 3-pt. flexure (span = 2.54 cm) and indented at 10 kg.

Batch A could not be tested for indented strength because of the warping and long cracks (10 mm in lengthwise direction). Batches B-D all showed warping with macropores ranging from 0.1-1 mm in size. These flaw sizes were measured by Chou using the SEM. These batches showed lenticular cracks. However, at high magnifications (1000X) the microstructures of samples C and D appear dense.

The observance of the lenticular cracks could be due to a variety of different factors. One reason is that there is too much polymer in the slurry. An overabundance of polymer could cause rebounding of the sample after it is released from the uniaxial press, thus leading to declamination which was a major source of critical flaw. The declamination of the sample is also possibly due to the preferential aligning of the tobermorite and xonotlite fibers or platelets. It was expected that the isostatic pressing would alleviate this problem but that is not the case. A third possible reason for delamination and the lenticular cracks could be that when the monomer starts to polymerize it pushes the cement particles apart or swelling of the polymer during curing in the water could push the cement particles apart.

The indented strengths of samples A-D were not as high as those achieved by MDF or DSP processing. This is due to the number and size of the flaws. The toughness, however,

is comparable to that of MDF or DSP cements. The lamination of the polymer in the isostatically pressed cement samples could be the reason for high toughness results.

Summary and Conclusions

Gel casting can be applied to cement using acrylamide as the monomer and potassium persulfate as the initiator. Acrylamide was chosen because polyacrylamide has been used successfully for conventional cements.

The forming technique used to produce the gel cast cements was isostatic pressing due to the higher pressures which could be achieved. Isostatic pressing also compacts the sample in three dimensions as opposed to two dimensions in uniaxial pressing.

The OPC samples which had the highest strength and toughness were those that were made using potassium persulfate, mixed with the Brabender (shear mixer) and cured in water. The samples made with the hydrothermally synthesized calcium silicate did not have high strength because of the lenticular cracks. These cracks are most probably caused by uniaxial pressing. Therefore, another shaping method will need to be evaluated in order to reduce the number and size of cracks in the final product.

Table 5: Summary of mechanical properties for samples A-D.

Sample	Density (g/cm^3)	% increase[1]	σ(MPa)	K_c(MPa $m^{1/2}$)
A[2]	1.8 ± 0.1	35.4	------	------
B	1.8 ± 0.1	35.3	26 ± 2	1.20 ± 0.1
C	2.1 ± 0.1	37.8	40 ± 2	1.40 ± 0.1
			58 ± 2	1.43 ± 0.1
D	2.1 ± 0.1	35.2	33 ± 2	1.24 ± 0.1

[1] After isostatic pressing

[2] Warping prevented measurements of strength and toughness

References

W.M. Kulicke, N. Bose, and M. Boulding, "The Role of Polymers in Enhanced Oil Recover," Water Soluble Polymers for Petroleum Recover, Eds. G.A. Stahl and D.N. Schulz (1988) 1-17.

Toyoichi Tanaka, "Gels," Scientific American 244 (1981) 124-155.

Y.S. Chou and J.J. Mecholsky, "Fracture of Chemically Derived, Chemically Bonded Ceramics," The Pennsylvania State University, Not yet published.

APPENDIX VIII

Kathleen Maes, Characterization and Use in Gel Casting Ssytems of Different Polyacrylamide Admixtures. Master of Science, Solid State Science, The Pennsylvania State University, defended August, 1991, approval by gradute school pending.

The Pennsylvania State University

The Graduate School

CHARACTERIZATION AND USE IN GEL CASTING SYSTEMS OF DIFFERENT POLYACRYLAMIDE ADMIXTURES

A Thesis in

Environmental Pollution Control

by

Katleen B. Maes

Submitted in Partial Fulfillment

of the Requirements

for the Degree of

Master of Science

December 1991

ABSTRACT

The in-situ polymerization of mono-functional and poly-functional monomers in aqueous solution is known as gel casting and is used to form ceramic bodies. In this study the monomeracrylamide, and the crosslinking agent N,'N Methylene-bis-acrylamide and the inorganic crosslinking agents (Na^+ and Ca^{2+}) were used in different concentrations and combinations to gel cast ground silica (quartz).

In the first part of the study the behavior of the polyacrylamide gel was examined. The influence of different crosslinking agents on the gel were determined by studying the following characteristics:

1. The heat production during the polymerization reaction was studied using an isothermal calorimeter.
2. The molecular structure of the polyacrylamide gels was studied using a Raman spectrometer.
3. The viscoelastic behavior of the polymer was studied through a series of creep-relaxation experiments.

These experiments show that the concentration of Ca^{2+} and Na^+ (pH of the aqueous solution) influences the heat production and the molecular structure more than the other tested variables. The heat production decreases when the pH increases. The Raman spectra show that with increasing pH, slight changes in the molecular structure occur. These differences in molecular structure cause a different viscoelastic behavior of the gels. Samples made with Na^+ are more anelastic, because the deformation of the formed chain entanglement in these samples is permanent. Because of their crosslinked structure, samples made with Ca^{2+} restore elastically to some extent after a stress has been applied.

The second part of the study tests the usefulness of these gels in gel casting ground silica solids.

Three aspects of the gel cast samples were studied: the tensile strength of the samples, the percent shrinkage after drying of the samples, and their micro-structures.

This study indicates crosslinking agents are useful to make three dimensional gels that can be used in gel cast systems to form brittle materials with a strength up to 6.46 MPa. Only a minor amount of crosslinking agent is needed, otherwise the gel becomes overcrosslinked, which decreases its elasticity.

TABLE OF CONTENTS

APPENDIX IX

K. Maes, M.R. Silsbee, B.E. Scheetz, J.H. Adair, and D.M. Roy, "Gel-Cast Organic-Inorganic Systems," accepted for publication in Proceedings of the Materials Research Society, 1991.

GEL-CAST ORGANIC-INORGANIC SYSTEMS

K. MAES, M.R. SILSBEE, B.E. SCHEETZ, J.H. ADAIR* and D.M. ROY
Materials Research Laboratory, The Pennsylvania State University, University Park, PA
*Materials Science and Engineering Department, University of Florida, Gainesvill,FL.

ABSTRACT

The studies reported herein were designed to develop a better understanding of the influence of different crosslinking agents on the polymerization of acrylamide gel systems and upon the resulting physical properties of the composites. Specimens were developed via a gel-casting process for viscoelastic and diametral tensile strength testing and the chemical reactions were monitored by Raman spectroscopy and isothermal calorimetry. The studies have demonstrated the ability to tailor the properties of a gel-cast system over a relatively wide range of reaction rates and the resulting mechanical properties by utilizing small adjustments to the overall chemistry of the system.

INTRODUCTION

Chemically bonded ceramics (CBC) are low-temperature materials, whose strength approaches those of many traditional high-temperature ceramics, and are a novel way of forming high strength ceramic materials. These materials are formed by a bonding that takes place via chemical reaction at low temperature, as opposed to fusion or sintering at elevated temperature. Gel-casting was chosen as the processing approach for this study, as it is envisioned to have potential application in cement solidification. In this process, the monomers and crosslinking agents are separately added to the ceramic (or cement) powder, mixed and the near final shaped object cast. The final step in the process is the induced polymerization of the monomer and crosslinking agents.

A major objective of this specific study was to develop a better understanding of the influence of different crosslinking agents on the polymerization of acrylamide and on the physical properties of the composite. The applications of these studies extends to such diverse fields as soil grouting systems [1], heavy metal stabilization and/or composite CBC products.

EXPERIMENTAL

The gel-casting process

Two monomers were used in this study: the di-functional monomer acrylamide (Am) and the di-functional monomer, N,N'methylene-bis-acrylamide (BisAAm). The acrylamide system was chosen for this study because its polymer has already been successfully used in MDF-cements prepared from ordinary portland cement (OPC) [2,3,4,5]. The crosslinking reaction utilized the BisAAm in order to create a three-dimensional structure. Additional crosslinking was obtained with metal ions Ca^{2+} and Na^{+}, which were added in the hydroxide form to the aqueous mixing

solution before polymerization. These ions were chosen to simulate contents of cement solutions. The basic aqueous solutions initiate in-situ polymerization [1] conversion of the carboxamide groups to carboxyl groups. Optimization of the crosslinking in the presence of inorganic cations is a function of pH, Eh and concentration [6,7]. The overall system must be carefully designed in order to avoid the gels becoming unstable and shrinking and to prevent syneresis.

Two types of samples were prepared for this study. One type consisted of just the polymerized acrylamide, the other a polymerized acrylamide with a ceramic filler. Both followed essentially the same preparation procedure with the former being prepared without the addition of the ceramic.

Characterization

Viscoelasticity is the time dependent change in stress at a constant deformation and temperature. To obtain these measurements, the gels, without ceramic addition, were placed between parallel plates and a load of 120g was applied to deform the gel. After a short period of time, long enough to stabilize the gel, the load was removed and the recovery of the gel monitored with an linear vector displacement transducer (LVDT). All displacement measurements were read directly into a computer and reported as the ratio of delta length change to length as a function of time.

The heats of polymerization were measured on a Seebeck isothermal calorimeter at 25^{o}C. All samples were run in a Teflon coated copper sample holder.

Changes in the vibrational spectra of the component acrylamide were monitored in the polymerized form with the different crosslinking agents on an Instruments SA Rananon U-1000 microfocus spectrometer. All data was collected with the 514 nm emission of argon ion laser set at 300mW of laser power. Spectra of all of the starting components were collected and served as "fingerprints" for comparison with the polymerized samples.

Simple strength tests were conducted with cylindrical specimens in a diametrical splitting configuration on an MTS load-frame using a 10,000 psi load cell. The crosshead speed was set at 0.002 inches per minute. Test specimens were prepared following the GEL-casting procedures outlined above. For this study, an inert filler consisting of approximately 70 weight percent 30 micron quartz was selected.

RESULTS AND DISCUSSION

Calorimetry

In this study, four different experiments were conducted to determine: a) the effect of varying amount of the BisAAm monomer upon crosslinking; b) the effect of varying amounts of Am and BisAAm on crosslinking; c) the effect of calcium ion with varying pH and d) the effect of sodium ion with varying pH. Compositions for specimens in these studies are presented in Table 1.

In general it was observed that as the amount of BisAAm and as the ratio of BisAAm to Am increased the degree of crosslinking as indicated by the enhanced liberation of heat. The rate of the chemical reaction as indicated by the time to reach maximum heat

TABLE 1. CHEMICAL FORMULATIONS USED IN EXPERIMENTS:
CALORIMETRIC VISCOELASTIC

Series	Chemical	Use	Concentration (Wt%)	Series	Concentration Wt%)
CAL-1.	Am	Monomer	3-34	VIS-1.	9.2
	BisAAm	Crosslinking	0.3-3.35		0.1-0.3
	Di	Agent	62.25-96.35		87.5-90.9
	Temed	Aqueous Solution	0.25		0.25
	$K_2S_2O_8$	Activator	0.4		0.38
		Initiator			
CAL-2.	Am	Monomer	34	VIS-2.	9.2
	BisAAm	Crosslinking	3.35		0.1
pH = 8-13	$Ca(OH)_2$+Di	Agent	62.25	pH = 11.46	90.2
	Temed	Aqueous Solution	0.25		0.26
	$K_2S_2O_8$	Activator	0.4		0.38
		Initiator			
CAL-3	Am	Monomer	34	VIS-3.	9.2
	BisAAm	Crosslinking	3.35		0.1
pH = 8-13	NaOH+Di	Agent	62.25	pH = 11.61	90.2
	Temed	Aqueous Solution	0.25		0.26
	$K_2S_2O_8$	Activator	0.4		0.38
		Initiator			
CAL-4.	Am	Monomer	34		
	BisAAm	Crosslinking	3-4		
	Di	Agent	62.25		
	Temed	Aqueous Solution	0.25		
	$K_2S_2O_8$	Activator	0.4		
		Initiator			

output also decrease monotonically with increasing crosslinking.

The presence of calcium ions in solution of varying pH appeared to have little effect upon degree of crosslinking across the pH range of 8 to 13. The rate of the reaction exhibited a decrease with increasing pH. This behavior is contrasted to the mono-valent cation, sodium which exhibited a marked decrease in heat liberation above about pH of 12. This behavior is mirrored by a sharp decrease in reaction rates in this same pH range. Figure 1 is presented as an example of these data.

Viscoelastic studies

Two sets of creep-relaxation experiments were performed in which a) gels with varying BisAAm concentrations and b) gels with Ca^{2+} and Na^{1+} concentrations were studied. These formulations are also presented in Table 1.

Results obtained in the experiments with constant concentrations of Am and varying amounts of BisAAm demonstrated that both maximum creep and maximum relaxation decreased with increasing BisAAm concentrations. These observations are in concert with intuitive assumptions that more crosslinking will result from greater concentrations of BisAAm and hence the gels will become more anelastic:

weight % BisAAm	0.1	0.5	1.0
creep/relaxation ratio	2.5	4.6	6.4

Polyacrylamide crosslinked with inorganic ions revealed markedly different effects. Samples prepared with sodium ions in solution exhibited a lower relative relaxation compared to a standard sample of gelled polyacrylamide without any cation addition, while gels with calcium ion, at the same concentration as sodium, exhibited a higher relative relaxation:

ion	none	Ca^{2+}	Na^{+}
creep/relaxation ratio	6.4	2.9	15.9

These results suggest that the chain branching caused by the

mono-valent sodium ion is greater than the di-valent calcium ion resulting in a stiffer more anelastic gel. This observation is consistent with what would be anticipated based solely on valence. The explanation of these observations lies in the nature of the chain entanglements that result for crosslinking. The sodium ions, having only a single charge, forms branches in the polyacrylamide molecules rather than extensive crosslinking networks. Charlesby [8] suggests that for a limited time period, chain entanglements behave as permanent crosslinks. Under stress, these chain entanglements undergo permanent changes. This interpretation is further supported by the behavior of the gels containing calcium. Here crosslinking networks are formed, so that when the outwardly applied stress is released, the network can restore itself to a greater extent than the entangled gels.

Raman spectroscopic characterization

Based on previous assignments [9,10,11,12] the Raman spectra of polyacrylamide gels crosslinked with sodium and calcium show changes in the skeletal stretching and skeletal deformation as the pH increased. The spectra in this region are very complex but maybe used as "fingerprints" to note changes. The most significant changes occurred in these spectra when the pH exceeded 12. However, when the fingerprint spectra of the sodium and calcium samples are contrasted, differences are present, suggesting significantly different crosslinking taking place. Although not fully interpretable in detailed terms, the Raman data both support the calorimetric and viscoelastic results.

Diametral tensile strength

Four separate sets of experiments were conducted with quartz filled, gel-cast polyacrylamide composites. These studies consisted of: a) varying the amount of BisAAm with constant Am and solids loading; b) varying the pH of aqueous solution containing sodium ions; c) varying the pH of aqueous solution containing calcium ions and d) varying the grain size of the inert filler. Table 2 details the composite conmpositions used in these studies.

Increasing the amount of BisAAm by just a half of a weight percent resulted in nearly a 50% decrease in strength from 6.5 MPa to about 3 MPa. The effects of both the calcium and sodium ions on the silica composites are quite similar. Optimum crosslinking appears to have occurred at pH of approximately 11.5 which is manifested in the maximum tensile strength of about 3.5 MPa. As the pH is varied from this optimal value the strengths of the composites are seen to decrease. The pH value of 11.5 is the value at which the onset of rapid decrease in the time to maximum heat production in the unfilled gels occurs. Finally, as would be anticipated, composites prepared with varying size fillers ranging from 5 to 30 microns exhibited a decreasing strength with increasing grain size, Table 2.

SUMMARY

The in situ polymerization and subsequent gelation of aqueous systems of organic monomers to bind inorganic matrixes has many applications. The objective of this study has been to examine the reactions occurring in and the characterization of one set of materials employing these methodologies. The results

of this study are intended to have more generic uses in a wide variety of applications. These studies have demonstrated the ability to tailor the properties of a gel cast system over a relatively wide range of reaction rates and the resulting mechanical properties by utilizing small adjustments to the overall chemistry of the system. This may be desirable in systems where precise control of these characteristics are required.

TABLE 2. FORMULATIONS USED IN GEL-CASTING EXPERIMENTS AND RESULTS OF TENSILE STRENGTH TESTS.

Iteration	Premix wt %					Initiator Solution Wt%			Solids		
	Am	BisAAm	DI	Temed	pH	$K_2S_2O_8$	DI	pH	wt% Ground Silica	Grainsize Micron	Average Samples +/-Sd Brittle
Bisacrylamide variable											
15	2.72	0.33	28.75	0.216	5.05	0.48	1.92	5.12	69.7	30	6.46 +/- 0.47
16	2.72	0.16	28.83	0.216	..	0.216	1.92	5.12	69.9	30	4.33 +/- 0.31
17	2.72	0.33	28.66	0.216	5.12	0.216	1.92	5.12	69.7	30	4.86 +/- 0.33
18	2.72	0.33	28.49	0.216	5.12	0.216	1.92	5.12	69.5	30	3.87 +/- 0.23
19	2.72	0.49	28.43	0.216	5.12	0.216	1.92	5.12	69.4	30	3.31 +/- 0.19
Methacrylamide sol.											
20	2.4	0.26	28.1	0.216	.. 91	0.22	1.92	11.61	71.3	30	3.23 +/- 1.68
21	2.4	0.26	28.1	0.216	12.65	0.22	1.92	10.63	69.7	30	3.26 +/- 0.21
24	2.4	0.26	28.1	0.216	9.38	0.22	1.92	9.38	69.7	30	3.89 +/- 0.22
Carbon sq. sol.											
23	2.4	0.26	28.5	0.216	.. 46	0.22	1.92	11.46	69.5	30	3.30 +/- 0.16
23	2.4	0.26	28.5	0.216	.. 21	0.22	1.92	10.21	69.5	30	3.17 +/- 0.21
25	2.4	0.26	28.5	0.216	9.03	0.22	1.92	9.03	69.5	30	3.89 +/- 0.28
Grainsize = variable											
33	2.72	0.33	25.53	0.216	5.12	0.216	1.92	5.12	69.5	30	3.57 +/- 0.23
36	3.12	0.33	28.20	0.216	5.12	0.216	1.92	5.12	69.11	10	4.65 +/- 0.3
34	3.27	0.26	30.73	0.216	5.12	0.216	1.92	5.12	69.24	5	5.83 +/- 0.75

However, these results also point to potential problems that may be encountered when utilizing these systems, that relatively small changes in concentrations and/or the presence of relatively small amounts of impurities may result in significant changes in characteristics of the composite.

ACKNOWLEDGEMENTS

The authors would like to acknowledge the financial support of the AFOSR by contract no. 88-0184 and the National Science Foundation by grant no. MSM-871811.

REFERENCES

[1] MacWilliams, D.C., Acrylamide and other alpha, beta unsaturated amides, in Functional Monomers, Marcel Dekker, Inc., New York, Eds. R.H. Yocum and E.B. Nyquist, 1-197 (1973).

[2] Roy, D.M., New strong cement materials: chemically bonded ceramics, Science, 235, 651-658 (1987).

[3] Silsbee, M.R., D.M. Roy and J.H. Adair, The chemistry of MDF cements produced from polyacrylamide-cement-waterpastes, Special cements with advanced properties, Ed. B.E. Scheetz, Materials Research Society, Vol 179, 129-144 (1990).

[4] Silsbee, M.R., M. Perez-Pena and D.M. Roy, A view of MDF pastes special cements with advanced properties, Ed. B.E. Scheetz, Materials Research Society, Vol 179, 145-158 (1990).

[5] Heiland, P.M., Processing and properties of chemically derived calcium silicate cement, M.S. Thesis, The Pennsylvania State University (1990).

[6] Conway, N.W., S.W. Almond, J.E. Briscoe and L.E. Harris, Chemical model for the rheological behavior of crosslinked fluid systems, J. Petr. Techn., 315-320 (1983).

[7] Menjivar, J.A., Use of gelation theroy to characterize metal crosslinked polymer gels, Adv. Chem. Series, 213, Am. Chem. Soc. Ed J.E. Glass, 209-226 (1986).

[8] Charlesby, A., Molecular weight changes and network formation by scission and crosslinking, Crosslinking and Scission in Polymers, Kluwer Academic Publisher, ed. O. Gueven, 1-13 (1990).

[9] Loy, B.R., R.W. Chrisman, R.A. Nyquist and C.L. Putzig, A Raman method for determining percent conversion of polyacrylamide to poly-N-dimethylamino-methylacrylamide, Appl. Spect.,33, 174-175 (1979).

[10] Gupta, M.K. and R. Bansil, Laser Raman spectroscopy of Polyacrylamide, J. Poly. Sc, Poly. Sc. Ed.19,353-360 (1981).

[11] Gupta, M.K. and R. Bansil, Raman spectroscopy as a structural probe of polyacrylamide gels, Poly. Prep. 22 192-193 (1981).

[12] Gupta, M.K. and R. Bansil, Raman spectroscopic and thermal studies of polyacrylamide gels with varying monomer/comonomer ratios, J. Poly. Sci. Poly. Lett..21, 969-977 (1983).

Figure 1. Reaction intensity for polyacrylamide gels (Am = 34 wt.%, BisAAm = variable). A) maximum peak heat B) time to reach the maximum peak heat for the different polymerization reactions. Part 1 - as function of BisAAm concentration. Part 2 - As function of pH (adjust with NaOH).